2007

Phosphatidylinositol 3-kinase activation is required to form the NKG2D immunological synapse

Emanuele Giurisato
Washington University School of Medicine in St. Louis

Marina Cella
Washington University School of Medicine in St. Louis

Toshiyuki Takai
Tohoku University

Tomohiro Kurosaki
RIKEN Research Center for Allergy and Immunology, Yokohama

Yungfeng Feng
Washington University School of Medicine in St. Louis

See next page for additional authors

Authors

Emanuele Giurisato, Marina Cella, Toshiyuki Takai, Tomohiro Kurosaki, Yungfeng Feng, Gegory D. Longmore, Marco Colonna, and Andrey S. Shaw

Phosphatidylinositol 3-Kinase Activation Is Required To Form the NKG2D Immunological Synapse

Emanuele Giurisato, Marina Cella, Toshiyuki Takai, Tomohiro Kurosaki, Yungfeng Feng, Gregory D. Longmore, Marco Colonna and Andrey S. Shaw
Mol. Cell. Biol. **2007, 27(24):8583. DOI: 10.1128/MCB.01477-07.**
Published Ahead of Print 8 October 2007.

MOLECULAR AND CELLULAR BIOLOGY, Dec. 2007, p. 8583–8599 Vol. 27, No. 24
0270-7306/07/$08.00+0 doi:10.1128/MCB.01477-07

Phosphatidylinositol 3-Kinase Activation Is Required To Form the NKG2D Immunological Synapse▽

Emanuele Giurisato,[1] Marina Cella,[1] Toshiyuki Takai,[2] Tomohiro Kurosaki,[3] Yungfeng Feng,[4] Gregory D. Longmore,[4] Marco Colonna,[1] and Andrey S. Shaw[1]*

Department of Pathology & Immunology, Washington University School of Medicine, St. Louis, Missouri 63110[1]; Department of Experimental Immunology, Institute of Development, Aging and Cancer, Tohoku University, Seiryo 4-1, Sendai 980-8575, Japan[2]; RIKEN Research Center for Allergy and Immunology, Laboratory for Lymphocyte Differentiation, 1-7-22 Suehiro-cho, Tsurumi-ku, Yokohama, Kanagawa 230-0045, Japan[3]; and Departments of Medicine and Cell Biology, Washington University, St. Louis, Missouri 63110[4]

Received 15 August 2007/Returned for modification 19 September 2007/Accepted 25 September 2007

The receptor NKG2D allows natural killer (NK) cells to detect virally infected, stressed, and tumor cells. In human cells, NKG2D signaling is mediated through the associated DAP10 adapter. Here we show that engagement of NKG2D by itself is sufficient to stimulate the formation of the NK immunological synapse (NKIS), with recruitment of NKG2D to the center synapse. Mutagenesis studies of DAP10 revealed that the phosphatidylinositol 3-kinase binding site, but not the Grb2 binding site, was required and sufficient for recruitment of DAP10 to the NKIS. Surprisingly, we found that in the absence of the Grb2 binding site, Grb2 was still recruited to the NKIS. Since the recruitment of Grb2 was dependent on phosphatidylinositol-(3,4,5)-trisphosphate (PIP_3), we explored the possibility that recruitment to the NKIS is mediated by a pleckstrin homology (PH) domain-containing binding partner for Grb2. We found that the PH domain of SOS1, but not that of Vav1, was able to be recruited by PIP_3. These results provide new insights into the mechanism of immunological synapse formation and also demonstrate how multiple mechanisms can be used to recruit the same signaling proteins to the plasma membrane.

Natural killer (NK) cells are important for the innate immune response against virally infected, stressed, and tumor cells (36, 41, 64). NK cell activation can elicit two different effector functions, namely, cytotoxicity of the target cell and/or secretion of cytokines and chemokines. NK cell activation is based on the integration of signals from activating receptors and inhibitory receptors (41, 56). Like those of other lymphoid cells, NK activating receptors can signal via immunoreceptor tyrosine-based activation motif (ITAM)-containing accessory chains, namely, DAP12, CD3ζ, and Fc receptor gamma (FcRγ). In humans, for example, activating killer cell immunoglobulin-like receptors, CD94/NKG2C-E, and the NKp44 natural cytotoxicity receptor associate with DAP12, while the NKp46 and NKp30 natural cytotoxicity receptors, as well as CD16, pair with CD3ζ and FcRγ (34).

Another important activating receptor used by NK cells is NKG2D, which is expressed on NK and T cells (50, 62). NKG2D recognizes ligands that are often induced due to the consequences of cellular stress, such as DNA damage, tumors, and viral infections (22). In humans, NKG2D ligands include major histocompatibility complex [MHC] class I chain-related (MIC) protein (1) and UL-16 binding protein (ULBP) (11). In mice, ligands for NKG2D include Rae1, H60, and MULT-1 (50).

In contrast to other NK activating receptors, human NKG2D is associated with DAP10, an accessory chain that does not contain an ITAM (21, 62). Consistent with this, the engagement of NKG2D by human NK cells can induce cytolytic activity but not cytokine production (2, 61, 65). Instead of an ITAM, DAP10 contains a signaling motif, YXNM, that is similar to motifs found in the costimulatory receptors CD28 and ICOS (27, 49). This raises questions about whether DAP10 functions independently or whether it functions in concert with other activating receptors. Supporting an independent signaling role for DAP10, a chimeric DAP10 construct was able to induce the tyrosine phosphorylation of a variety of substrates (2).

DAP10 can potentially signal by becoming phosphorylated and associating with both the p85 subunit of phosphatidylinositol 3-kinase (PI 3-kinase) and the adapter protein Grb2 (8, 62). In addition, it has been shown that NKG2D stimulation can induce the phosphorylation of JAK2, STAT5 (55), Itk (32), extracellular signal-regulated kinase (ERK) (39, 55), Vav1 (2, 7), and Jun N-terminal kinase (39). Recently, Leibson and coworkers found that the recruitment of both p85 and a Grb2-Vav1 complex is required for NK lytic activity (59).

Recognition of target cells requires the formation of a structure called an NK cell immunological synapse (NKIS) at the contact site (4, 14, 15). Two forms of synapses have been described for NK cells, namely, the activating and the inhibitory NKIS (13, 38, 58, 60). NKG2D engagement is known to be able to induce the formation of an immunological synapse in $CD8^+$ T cells (37, 53). These synapses are remarkable for the clear segregation of the integrin LFA-1 in an outer zone called the peripheral supramolecular activation cluster (pSMAC) and for the clustering of NKG2D in a central zone called the central supramolecular activation cluster (cSMAC) (4). Although NKG2D has been observed to accumulate at the con-

* Corresponding author. Mailing address: Department of Pathology & Immunology, Washington University School of Medicine, St. Louis, MO 63110. Phone: (314) 362-4614. Fax: (314) 747-4888. E-mail: shaw@pathology.wustl.edu.

▽ Published ahead of print on 8 October 2007.

tact site between NK cells and NKG2D ligand-expressing target cells (17, 19, 42, 52), the signaling mechanisms involved in formation of the activating NKIS and the types of synapses generated by NKG2D in NK cells are not known (4, 15).

Here we investigated the roles of NKG2D and DAP10 in NK cell synapses. Using a model system, we show that NKG2D can generate an NKIS on its own, without the requirement for any other NK cell activating receptor. This allowed us to determine which structural elements in DAP10 are required for NKG2D-mediated synapse formation. We found that the PI 3-kinase binding site, but not the Grb2 binding site, was critical for DAP10 recruitment to the contact site. Surprisingly, abrogating Grb2 binding to DAP10 did not block recruitment of Grb2 to the NKIS. Instead, we found that Grb2 recruitment was PI 3-kinase dependent. Since Grb2 is known to associate with both SOS1 (9) and Vav1 (46), which both contain pleckstrin homology (PH) domains, we tested each for the ability to be recruited to the NKIS by phosphatidylinositol-(3,4,5)-trisphosphate (PIP_3). We found that the PH domain of SOS1, but not that of Vav1, was able to be recruited by PIP_3. These results provide new insights into the mechanism of immunological synapse formation and also demonstrate how multiple mechanisms can be used to recruit the same signaling proteins to the plasma membrane.

MATERIALS AND METHODS

Cells lines and antibodies. Human interleukin-2 (IL-2)-dependent NK92 cells were kindly provided by M. J. Robertson and were grown in RPMI 1640 medium supplemented with 10% fetal bovine serum (FBS) and 100 U/ml of human IL-2 (hIL-2). P815 murine mastocytoma cells and human Daudi B lymphoma cells were grown in RPMI 1640 medium supplemented with 10% FBS. ULBP1-expressing P815 cells were grown in RPMI 1640 medium supplemented with 10% FBS containing 1 mg/ml of G418 sulfate (Gibco). Human NK cells were purified by $CD56^+$ magnetic cell sorting enrichment (Miltenyi) following Ficoll gradient centrifugation of buffy coats and were grown in hIL-2-containing medium. Monoclonal anti-hNKG2D was obtained from R&D Systems. Goat anti-mouse immunoglobulin G (IgG) conjugated to allophycocyanin (Molecular Probes), biotinylated anti-human CD8α (eBioscience), streptavidin-phycoerythrin (PE)-Cy5 (Pharmingen), and mouse anti-SOS1 (BD Transduction Laboratories) were also used. NKG2D tetramer-streptavidin-PE was kindly provided by D. H. Fremont.

Generation of DNA constructs. Murine DAP10 or DAP12 full-length cDNA was amplified by reverse transcription-PCR from mouse RNA and subcloned into the pEYFP-N1 vector (Clontech). DNA encoding the PH domain of Akt [PH(Akt); a gift from G. Longmore] was subcloned into the pEGFP-N1 vector (Clontech). After EcoRI and NotI digestion, DAP10-yellow fluorescent protein (DAP10-YFP), DAP12-YFP, and PH(Akt)-green fluorescent protein [PH(Akt)-GFP] were cloned into the pMX retrovirus vector (45). The Y72F, N74Q, and M75V mutations in the YINM motif of DAP10-YFP were generated using PCR site-directed mutagenesis (Stratagene). The primers used for the Y72F mutation were 5′-AGA GTC TTC ATC AAC ATG CCT GGC AGA GGC-3′ and 5′-GTT GAT GAA GAC TCT ACC ATC TTC TTG GGC-3′, those used for the N74Q mutation were 5′-AGA GTC TAC ATC CAA ATG CCT GGC AGA GGC-3′ and 5′-AGG CAT TTG GAT GTA GAC TCT ACC ATC TTC-3′, and those used for the M75V mutation were 5′-GGT AGA GTC TAC ATC AAC GTA CCT GGC AGA GGC-3′ and 5′-TCT GCC AGG TAC GTT GAT GTA GAC TCT ACC ATC-3′. A cDNA containing the human CD8α leader segment followed by the Flag epitope coding sequence (35) was used to create a Flag-tagged CD8-DAP10 chimeric construct carrying the human CD8α chain extracellular and transmembrane domains and the cytoplasmic region of mouse DAP10 (amino acids 52 to 80). The Flag-CD8-DAP10 cDNA was subcloned into the pMX retrovirus vector, and mutations in the YINM motif of DAP10 were generated as described above.

Human Grb2 full-length cDNA was amplified by PCR and fused with a monomeric DsRed fluorescent protein (6). After BamHI and NotI digestion, DsRed-Grb2 was cloned into the pMX retrovirus vector. A plasmid containing human SOS1 was a gift from D. Bar-Sagi. The sequence encoding the PH domain of SOS1 (amino acids 422 to 551) was PCR amplified and subcloned into the pEGFP-N1 vector and, after BamHI digestion, the pMX vector. The retroviral expression vector containing Vav1-GFP was provided by W. Swat. The R422G and K404A mutants of the PH domain of Vav1 (26) were generated using PCR site-directed mutagenesis (Stratagene). DNA encoding the human Vav1 PH domain (amino acids 347 to 449) was PCR amplified and subcloned into the pEGFP-N1 vector, and after EcoRI/NotI digestion, PH(Vav1)-GFP was cloned into the pMX vector. The retroviral expression vector containing mouse CD3ζ-GFP was provided by M. M. Davis (51). The integrity of all constructs was confirmed by automated sequencing.

RNA interference. Grb2 small hairpin RNA (shRNA) and luciferase (control) shRNA constructs were generated using a multifunctional lentivirus system (with the pFLRu lentivector provided by Y. Feng and G. D. Longmore). The targeting sequence for human Grb2 (DNA fragment nucleotides 609 to 627) used to generate the Grb2 shRNA construct has been described previously (29). XbaI-digested Vav1-GFP was subcloned into luciferase and Grb2 shRNA vectors to create pFLRu-(luciferase-shRNA)-Vav1-GFP and pFLRu-(Grb2-shRNA)-Vav1-GFP, respectively. For lentivirus production, subconfluent cultures of 293T cells were transfected with a packaging plasmid (pHR′8.2deltaR/pCMV-VSV-G at a ratio of 8:1) and a pFLRu-derived plasmid (Y. Feng, H. Zhao, B. Wang, and G. D. Longmore, submitted for publication). The integrity of all constructs was verified by automated sequencing. The lentivirus infection of NK92 cells was performed using a previously described protocol (40). NK92/luciferase-shRNA-Vav1-GFP cells and NK92/Grb2-shRNA-Vav1-GFP cells expressing the same level of Vav1-GFP were sorted 7 to 10 days later on a Beckton Dickinson FACSVantage SE flow cytometer at the Flow Cytometry Core Facility, Department of Pathology and Immunology, Washington University, St. Louis, MO.

Confocal imaging and immunofluorescence staining. NK92 cells transduced with a retroviral expression vector encoding DAP10 (NK92/DAP10-YFP), DAP12 (NK92/DAP12-YFP), CD3ζ (NK92/CD3ζ-GFP), PH(Akt)-GFP [NK92/PH(Akt)-GFP], PH(Vav1)-GFP, or PH(SOS1)-GFP were mixed with P815, P815-ULBP, or Daudi B cells at a 1:1 ratio and placed in parallel-plate flow cells in a temperature-controlled chamber at 37°C. Where indicated, transduced NK92 cells were loaded with 100 nM Lysotracker (Molecular Probes) at 37°C for 30 min, with or without 100 nM wortmannin (WTN; Sigma). Images were taken over a period of 0 to 15 min, using a Zeiss LSM 510 laser scanning confocal microscope (Oberkochen, Germany) with a 63× objective lens. To study the recruitment of DAP10-YFP to the NKIS, NK92 cells expressing wild-type (WT) or mutant DAP10-YFP were mixed with an equal amount of the indicated target cells. After centrifugation, cells were gently resuspended and placed onto poly-L-lysine-coated glass slides for 30 min at 37°C. After the medium was aspirated, cells were fixed with 4% paraformaldehyde in phosphate-buffered saline for 10 min. Where indicated, NK92/DAP10YFP (WT) cells were pretreated with 100 nM WTN for 30 min at 37°C. We examined ≥40 cells per slide. To study the recruitment of Grb2 to the contact site, NK92 cells coexpressing PH(Akt)-GFP and DsRed-Grb2 were incubated with the indicated target cells, as described above, for 15 min at 37°C and then fixed. Where indicated, transduced NK92 cells were pretreated with 100 nM WTN for 30 min at 37°C. To stain for Vav1, F-actin, or Grb2 accumulation, cells were permeabilized with 0.05% Triton X-100 and incubated with Alexa Fluor 568-phalloidin (Molecular Probes), mouse anti-Vav1 (Chemicom), or mouse anti-Grb2 (Santa Cruz) followed by Cy3-labeled goat anti-mouse (Jackson ImmunoResearch Laboratories). To test the DAP10 sequence requirements for Grb2 recruitment to the contact site, P815 target cells were preloaded with mouse anti-Flag M2 (10 μg/ml) for 30 min at 4°C. After being washed, target cells were incubated with NK92/Flag-CD8-DAP10 cells coexpressing PH(Akt)-GFP and DsRed-Grb2 at a 1:1 ratio, centrifuged, placed onto poly-L-lysine-coated glass slides for 15 min at 37°C, and fixed. To quantitate the recruitment of DAP10-YFP, DAP12-YFP, CD3ζ-GFP, and F-actin to the NKIS, boxes were drawn at the contact area between the NK and target cells, at the cell membrane not in contact with the target, and in a background area outside the cell, using the Image J software program (NIH). The relative recruitment index (RRI) was calculated as follows: (mean fluorescence intensity [MFI] at synapse − background MFI)/(MFI at regions not in contact with target cell − background MFI). For each experiment, the percentage of NK cells with RRIs of >1.2 was calculated. For quantification of PH(Akt)-GFP, PH(Vav1)-GFP, PH(SOS1)-GFP, Grb2, and Vav1 translocation to the NK cell contact area, the ratio of the MFI at the contact area to that in the cytosol was calculated, and ratios of >1.2 were scored as protein accumulation. At least 50 conjugates were examined for each experiment for a total of three different experiments.

Retroviral transduction of NK92 cells. The Phoenix amphotropic retroviral packaging cell line was kindly provided by Garry Nolan. After transfection using Lipofectamine 2000 (Life Technologies), cells were transferred to 32°C to allow

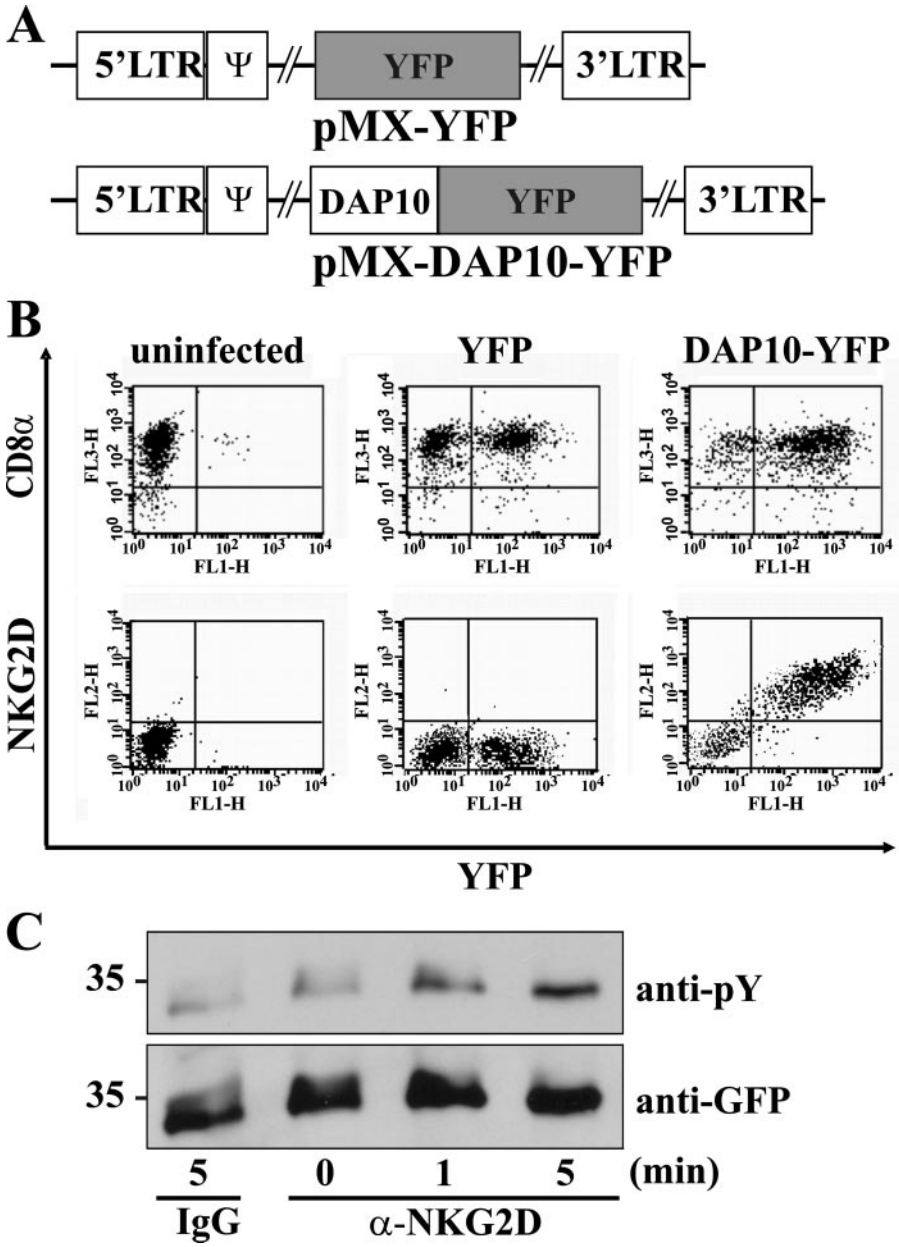

FIG. 1. Functional characterization of DAP10-YFP chimeras. (A) Schematic depiction of DAP10-YFP constructs used. LTR, long terminal repeat. (B) Rescue of NKG2D expression with DAP10 chimeras. Purified $CD8^+$ T cells from DAP10/$DAP12^{ko}$ mice were retrovirally transduced with the indicated constructs. The surface expression of CD8α and NKG2D was assessed by staining with specific antibodies and analyzed by fluorescence-activated cell sorting. (C) NKG2D engagement-induced DAP10-YFP phosphorylation. Sorted NK92/DAP10-YFP cells were IL-2 starved and stimulated with mouse anti-human NKG2D-coated beads or mouse IgG-coated beads for the indicated times. NK cell lysates were resolved by SDS-PAGE, transferred to nitrocellulose, and immunoblotted with anti-phosphotyrosine 4G10 (anti-pY) (top) or polyclonal rabbit anti-GFP (bottom).

accumulation of virus in the supernatant. Virus-containing supernatant was harvested 24 and 48 h after transfection and filtered through 0.45-μm syringe filters (Millipore). NK92 cells were incubated with viral supernatant in the presence of 8 μg/ml of Polybrene (Sigma) and then centrifuged at 900 × *g*. This step was repeated after 4 h. Cells expressing YFP, GFP, and/or DsRed were sorted 4 to 6 days later.

Retroviral transduction of $CD8^+$ T cells. Splenic $CD8^+$ T cells from DAP10/$DAP12^{ko}$ mice (31) were purified by positive selection with $CD8^+$ T-cell biotin-antibody cocktail microbeads (Miltenyi Biotech). Plat-E packaging cells were grown in RPMI 1640 medium supplemented with 10% FBS, 10 μg/ml puromycin (Sigma), and 10 μg/ml Blasticidin (Invitrogen). Plat-E cells were transfected as described above. Virus-containing medium was filtered and added to $CD8^+$ T-cell blasts from DAP10/$DAP12^{ko}$ mice 18 h after stimulation with anti-CD3 (2C11; 1 μg/ml) plus anti-CD28 (0.5 μg/ml) antibody. The mixture was centrifuged at 900 × *g* in the presence of 4 μl/ml of Lipofectamine 2000. After 48 h, $CD8^+$ T cells were stained with PE–Cy5–anti-CD8α and PE–anti-NKG2D antibody (Pharmingen, San Diego, CA).

Lipid bilayers. Biotinylated liposomes were made as described previously (25). Glycosylphosphatidylinositol-anchored ICAM-1 labeled with Cy5–*N*-hydroxysuccinimide (Amersham Biosciences) was incorporated into liposomes as described previously (25). Planar bilayers were made by mixing the ICAM-1-containing liposomes and the biotinylated liposomes at a ratio of 1:1 on clean

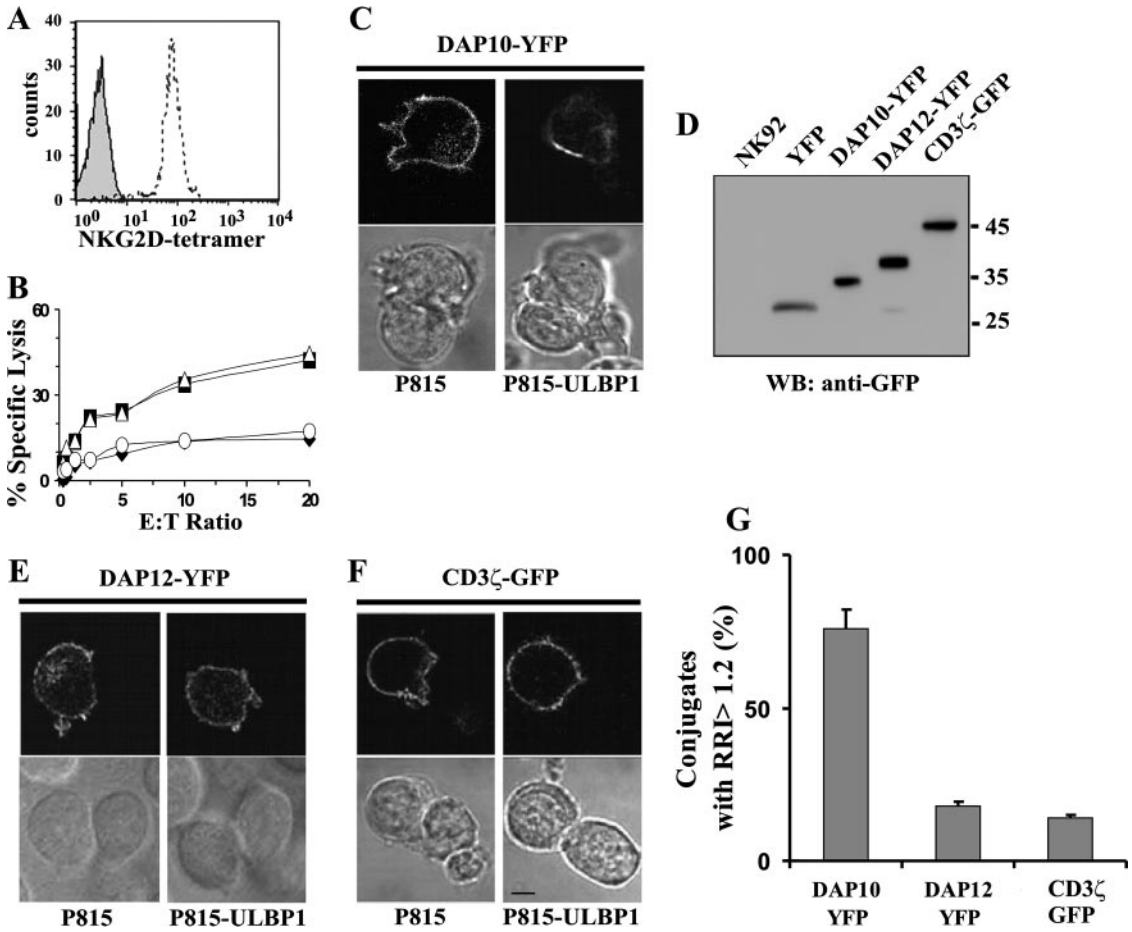

FIG. 2. Recruitment of DAP10-YFP to the NKIS does not require ITAM-containing adapter molecules. (A) Staining of P815 cells (gray profile) and P815-ULBP1 cells (dotted line) with NKG2D tetramer-streptavidin-PE. (B) NKG2D-mediated cytotoxicity activity. NK92 cells were incubated at the indicated effector/target (E:T) ratios with ^{51}Cr-labeled P815 cells (closed diamonds) or ^{51}Cr-labeled P815-ULBP1 cells before (closed squares) or after preincubation with streptavidin-PE (open triangle) or NKG2D tetramer-streptavidin-PE (open circles). Data are representative of five different experiments. (C) DAP10-specific recruitment by NKG2D ligand. Target cells and effector cells were incubated together at 37°C, and live confocal images were collected 0 to 15 min after cell mixing. Representative differential interference contrast (DIC) and YFP fluorescence images are shown for cells expressing DAP10-YFP conjugated to P815 (left) or P815-ULBP1 (right) target cells. (D) Protein expression levels of NK92 stable cell lines transduced with YFP (lane 2), DAP10-YFP (lane 3), DAP12-YFP (lane 4), or CD3ζ-GFP (lane 5) were determined by immunoblotting (WB) using rabbit anti-GFP. (E and F) Representative DIC and YFP fluorescence images are shown for cells expressing DAP12-YFP (E) or CD3ζ-GFP (F) conjugated to P815 (left) or P815-ULBP1 (right) target cells. Bar, 5 μm. (G) Quantitative analysis of DAP10, DAP12, and CD3ζ accumulation at the NKIS. The RRI (see Materials and Methods) represents the mean of at least 30 conjugates from three independent experiments. Error bars show standard deviations.

glass coverslips in a flow cell (Bioptechs). Streptavidin-Alexa Fluor 488 (Molecular Probes) was flowed (1 μg/ml) over the bilayer, followed by a wash with HEPES-buffered saline (HBS). Biotinylated Rae1ε (1 μg/ml; kindly provided by D. H. Fremont) was then flowed over the bilayer, followed by a wash with HBS. Cells were then injected into the flow cell in HBS containing 1% human serum albumin (Alpha Therapeutic). Cells were imaged using a Zeiss LSM 510 confocal system (Oberkochen, Germany) with a 63× objective lens. All images of cells on bilayers were taken with the pinhole open over a period of 0 to 30 min.

Cytotoxicity assays. Cytotoxic activity of NK92 cells was tested against target cells by using a standard 4-h ^{51}Cr release assay (7). Where indicated, P815-ULBP1 or Daudi B cells were pretreated with NKG2D tetramer-streptavidin-PE (1 μg/ml) or with streptavidin-PE (1 μg/ml) at room temperature for 15 min. In redirected killing assays, the FcR$^+$ P815 target cells were first incubated with mouse anti-Flag M2 (10 μg/ml) for 30 min at 4°C. After being washed, target cells were incubated with various mutants of NK92/Flag-CD8-DAP10 cells. In all experiments, spontaneous release did not exceed 10% of maximum release.

Cell conjugation assay. Target cells were preincubated with CellTrace red-orange AM (Molecular Probes) at 1 μM for 15 min at 37°C. After being washed, NK92/PH(Akt)-GFP cells were incubated with CellTrace-loaded target cells at a ratio of 1:1 for 20 min at 37°C. Conjugate formation was monitored by flow cytometry. Where indicated, NK92/PH(Akt)-GFP cells were preincubated with 100 nM WTN for 30 min at 37°C.

Cell stimulation, immunoprecipitation, and immunoblotting. NK92 cells (5×10^6/sample) transduced with WT DAP10-YFP and DAP10-YFP mutants were IL-2 starved for 4 h in RPMI 1640 containing 5% FBS. Cells were incubated with anti-human NKG2D-coated beads or with mouse IgG-coated beads at 37°C for the indicated times. After stimulation, the pellet was resuspended in ice-cold lysis buffer (0.1 M Tris base, 140 mM NaCl, 1 mM EDTA containing 1% NP-40, 1 mg/ml apoprotein, 1 mM phenylmethylsulfonyl fluoride, 1 mM sodium orthovanadate, and 50 mM sodium fluoride). After centrifugation, nucleus-free supernatant was incubated with 2 μg/ml of polyclonal anti-GFP and then incubated with protein A-Sepharose beads (Pharmacia) at 4°C for 90 min. After being washed, GFP immunoprecipitates were resolved by sodium dodecyl sulfate-polyacrylamide gel electrophoresis (SDS-PAGE), transferred to a membrane, and probed with a monoclonal antibody (MAb) to phosphotyrosine 4G10 (Upstate), polyclonal rabbit anti-GFP (Invitrogen), or polyclonal rabbit anti-Grb2 (Santa Cruz), followed by incubation with anti-mouse IgG or anti-rabbit IgG coupled to horseradish peroxidase. For detection of the SOS1-Grb2-Vav1

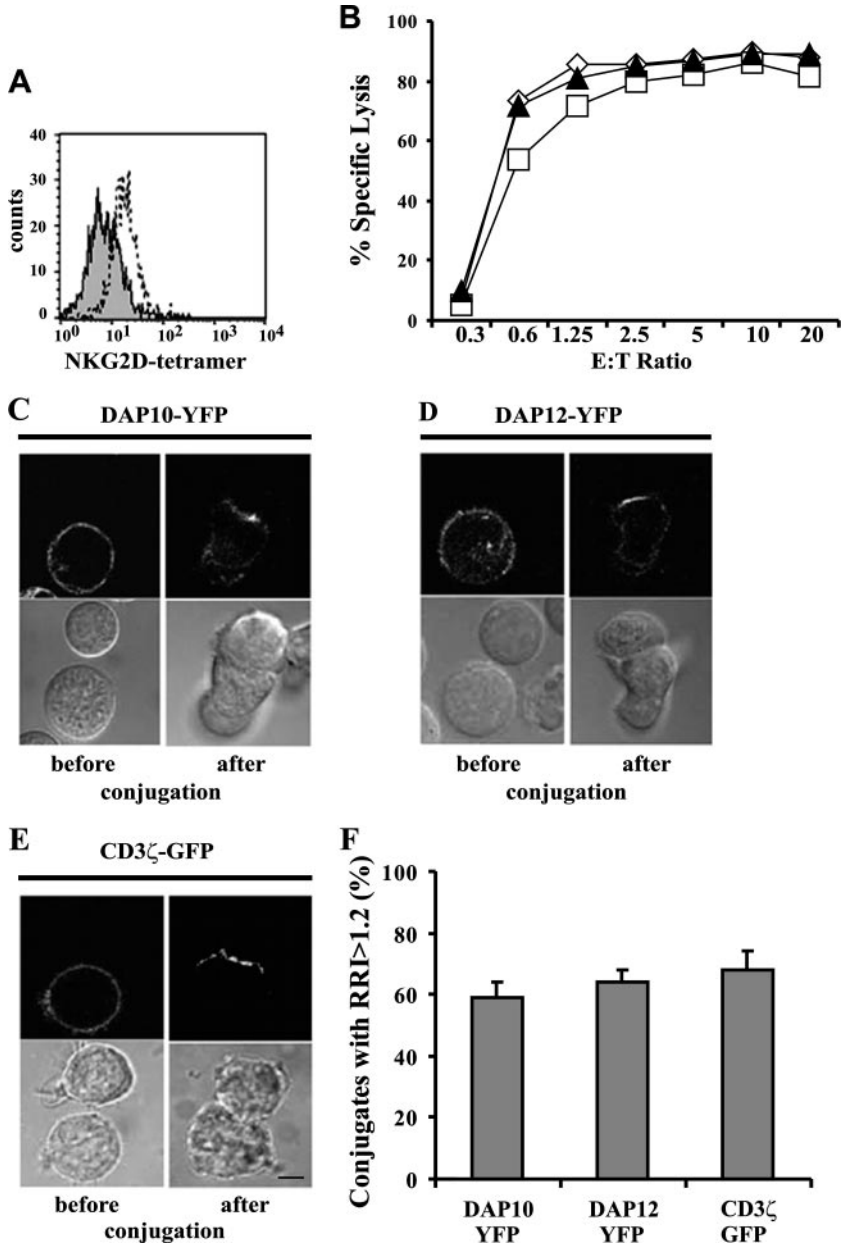

FIG. 3. Recruitment of chimeric DAP10, DAP12, and CD3ζ proteins to the NKIS. (A) Expression of NKG2D ligands on Daudi B cells, as determined by specific staining using NKG2D tetramers (dotted line). Control staining with streptavidin-PE alone is shown by the gray profile. (B) NK92 cell killing of Daudi cells is not blocked by NKG2D tetramers. NK92 cells were incubated at the indicated effector/target (E:T) ratios with ^{51}Cr-labeled Daudi cells (closed triangles) or ^{51}Cr-labeled Daudi cells preincubated with NKG2D tetramers (open squares) or streptavidin-PE alone (open diamonds). After 4 h at 37°C, the amounts of ^{51}Cr released into the supernatants were measured. Data are representative of five different experiments. (C to E) Imaging of recruitment of DAP10, DAP12, and CD3ζ after conjugation with Daudi B cells. Transduced NK92 cells were mixed with Daudi B cells and incubated at 37°C, and confocal images were collected 0 to 15 min after cell mixing. Representative DIC and YFP fluorescence images of a single 1-μm plane are shown for DAP10-YFP (C), DAP12-YFP (D), and CD3ζ-GFP (E) before (left) and after (right) conjugation with the indicated target cells. Bar, 5 μm. (F) Quantitation of DAP10, DAP12, and CD3ζ accumulation at the NKIS. The RRI represents the mean of at least 30 conjugates from three independent experiments. Error bars show standard deviations.

interaction, 1.0×10^7 IL-2-starved NK92/luciferase-shRNA-Vav1-GFP cells or NK92/Grb2-shRNA-Vav1-GFP cells were lysed in 2 ml of ice-cold lysis buffer containing 0.1% Nonidet P-40 buffer and then centrifuged as described above. The nucleus-free supernatant was divided into 1-ml aliquots, immunoprecipitated for 2 h with anti-SOS1 or IgG, and then incubated with protein A-Sepharose beads (Pharmacia) at 4°C for 90 min. After being washed, immunoprecipitates were analyzed by immunoblotting with the indicated antibody. To analyze ERK1/2 and Akt phosphorylation, NK92 cells or CD56$^+$ human primary NK cells were IL-2 starved, preincubated with or without WTN at 37°C for 30 min, and stimulated as described above. Proteins from cell lysates were analyzed by immunoblotting with antibodies specific for phosphorylated ERK [pERK1/2 (Thr202/Tyr204); Cell Signaling Technology], phosphorylated Akt [pAkt (Ser473); Cell Signaling Technology], phosphorylated Lck (pY394Lck), and ERK2 (Santa Cruz). Polystyrene microspheres (4.5 μm; Polysciences) were coated with mouse anti-human NKG2D MAb (5 μg/ml) or with mouse IgG (5 μg/ml) in phosphate-buffered saline.

RESULTS

Characterization of DAP10-YFP chimeras. To study the dynamics of DAP10 in living cells, YFP was fused to the C terminus of DAP10 (Fig. 1A). To confirm that the DAP10-YFP chimera was functionally active, we tested whether expression of the chimera in DAP10/DAP12-deficient $CD8^+$ T cells could rescue NKG2D expression (Fig. 1B). Retroviral transduction of DAP10-YFP expression rescued NKG2D surface expression, establishing that the DAP10-YFP chimera can associate with endogenous NKG2D (Fig. 1B). This was specific, because transduction with YFP by itself was unable to rescue expression of NKG2D on the cell surface (Fig. 1B).

We next confirmed that tyrosine phosphorylation of the DAP10-YFP chimera could be induced by engagement of NKG2D. The hIL-2-dependent transformed cell line NK92 was retrovirally transduced with the DAP10-YFP chimera (NK92/DAP10-YFP cells) and incubated with anti-NKG2D-coated beads. Immunoblotting demonstrated that tyrosine phosphorylation of DAP10-YFP was induced (Fig. 1C). In contrast, no phosphorylation was detected after incubation with mouse control IgG-coated beads (Fig. 1C). These results establish that the attachment of YFP to DAP10 does not interfere with its function.

Specific recruitment of DAP10 to the NKIS. To study the recruitment of DAP10 to the NKIS, we used P815 cells as target cells, as they do not express any ligands for NKG2D (Fig. 2A, gray profile). To allow for NKG2D recognition, P815 cells were transfected with the human NKG2D ligand ULBP1 (P815-ULBP1 cells) (Fig. 2A, dotted line). As expected, expression of ULBP1 on P815 cells conferred cytolytic killing by the NK92 cell line (Fig. 2B, closed squares). This was specific to NKG2D, as killing was blocked by the addition of NKG2D tetramers (Fig. 2B, open circles).

We next analyzed the localization of DAP10-YFP during the engagement of NKG2D by ligand, using confocal microscopy. In the absence of ULBP1, DAP10-YFP did not accumulate at the contact site (Fig. 2C, left panels). In contrast, incubation with P815-ULBP1 cells induced recruitment of DAP10-YFP to the NKIS (Fig. 2C, right panels, and G).

To determine whether DAP10 recruitment to the NK synapse was independent of ITAM-containing receptors, chimeric constructs of CD3ζ and DAP12 fused to YFP were generated (Fig. 2D) and imaged after conjugate formation with P815-ULBP1 cells. DAP12 associates with the NK activating receptors NKp44, KIR2/3DS, and CD94/NKG2C-E (57), while CD3ζ associates with the NK activating receptors NKp30, NKp46, and FcγRIII (CD16) (34). No detectable recruitment of CD3ζ or DAP12 to the NKIS was seen after incubation with ULBP1-expressing cells (Fig. 2E to G). Importantly, we confirmed the ability of DAP12 and CD3ζ fusion proteins to be recruited to the NKIS by incubating transduced NK92 cells with Daudi cells, which express ligands for a variety of activating receptors, including NKG2D (48) (Fig. 3A), and therefore are killed by NK92 cells (Fig. 3B). After conjugation with Daudi cells, all three adapter molecules were recruited to the contact site (Fig. 3C to F). The specific recruitment of DAP10 to the NKIS by ULBP1 supports the idea that NKG2D signaling is mediated exclusively by DAP10 in NK92 cells and does not require the cooperation of an ITAM-dependent activating receptor.

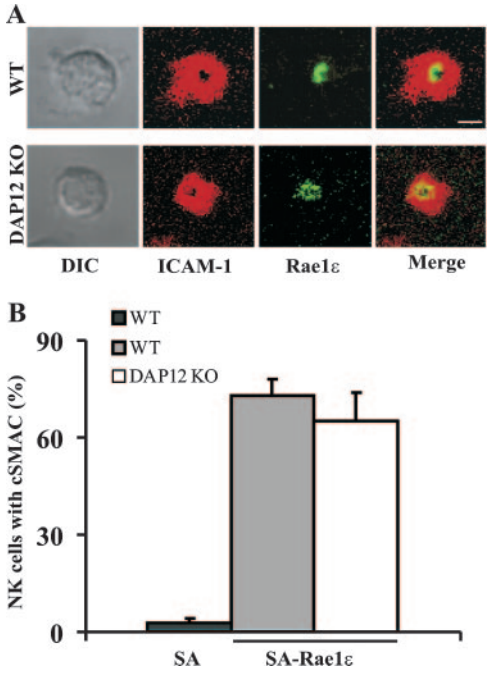

FIG. 4. NKG2D recruitment to cSMAC is independent of other NK receptor ligands. (A) NKG2D-dependent cSMAC formation on artificial lipid bilayers. $NK1.1^+$ $CD3^-$ cells from WT or DAP12-deficient (DAP12 KO) C57BL/6 mice were incubated on a lipid bilayer containing glycosylphosphatidylinositol-linked ICAM-1–Cy5 (red) and streptavidin-Alexa Fluor 488 (green), with or without biotinylated Rae1ε. Bar, 5 μm. (B) Percentage of NK cells forming cSMAC in the absence (SA) or presence (SA-Rae1ε) of 1 μg/ml Rae1ε on the lipid bilayer. Data are representative of three independent experiments. Error bars show standard deviations. In each case, over 50 cell contacts were analyzed to generate the graph.

We confirmed that NKG2D recruitment is independent of other NK cell receptors by imaging mouse NK cells plated on an artificial lipid bilayer containing fluorescently labeled Rae1ε (a mouse NKG2D ligand) and ICAM-1 (the ligand for LFA-1) (18, 25). Mouse NK cells plated on these bilayers quickly stopped and formed synapses, seen as a peripheral ring of ICAM-1 surrounding a central cluster of Rae1ε (Fig. 4A). No obvious synapse formation was observed in the absence of NKG2D ligand, as NK cells failed to stop (Fig. 4B). Since in mouse NK cells NKG2D can be associated with either the DAP10 or DAP12 adapter molecule (16, 23), we used NK cells from DAP12-deficient mice (31). Central clustering of Rae1ε using DAP12-deficient NK cells was similar to that of WT cells, indicating that DAP10 alone is sufficient for NKG2D recruitment to the synapse. These data support our finding that induction of the NKIS by NKG2D engagement can be mediated by signals transduced by DAP10 alone and is independent of ITAM-containing receptors.

Residues required for recruitment of DAP10 to the NKIS. DAP10 contains only a short cytoplasmic domain that is notable for a motif containing the sequence YINM (Fig. 5A). To determine which aspects of this motif are required for DAP10 recruitment to the NKIS, three mutated constructs were gen-

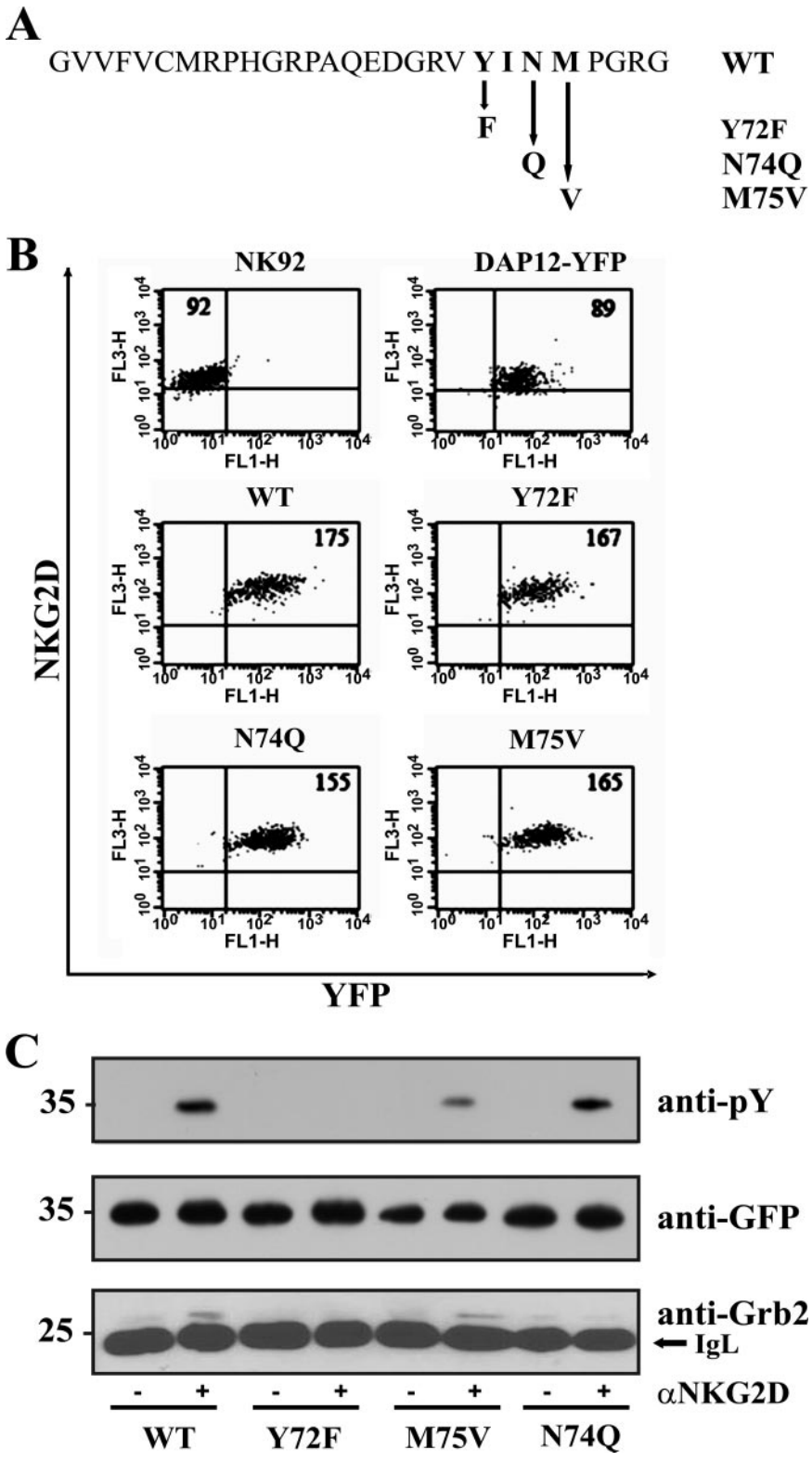

FIG. 5. Analysis of DAP10-YFP mutants. (A) The amino acid sequence of the mouse DAP10 cytoplasmic tail and mutated residues are shown using the one-letter amino acid code. (B) Cell surface expression of NKG2D on NK92 cells transduced with WT DAP10-YFP or the Y72F, N74Q, or M75V mutant DAP10-YFP chimera after being sorting for NKG2D and YFP expression. Transduction with DAP12-YFP alone was used as a control. Numbers represent the MFIs of NKG2D staining. (C) N74 residue of DAP10 is required for Grb2 binding. NK92 cells transduced with WT or mutant DAP10-YFP were stimulated with mouse anti-NKG2D-coated beads (+) or with mouse IgG-coated beads (−) for 5 min. DAP10-YFP immunoprecipitates were resolved by SDS-PAGE and probed with a MAb to phosphotyrosine (4G10; anti-pY) or with anti-Grb2. The membrane was then stripped and reprobed with polyclonal rabbit anti-GFP.

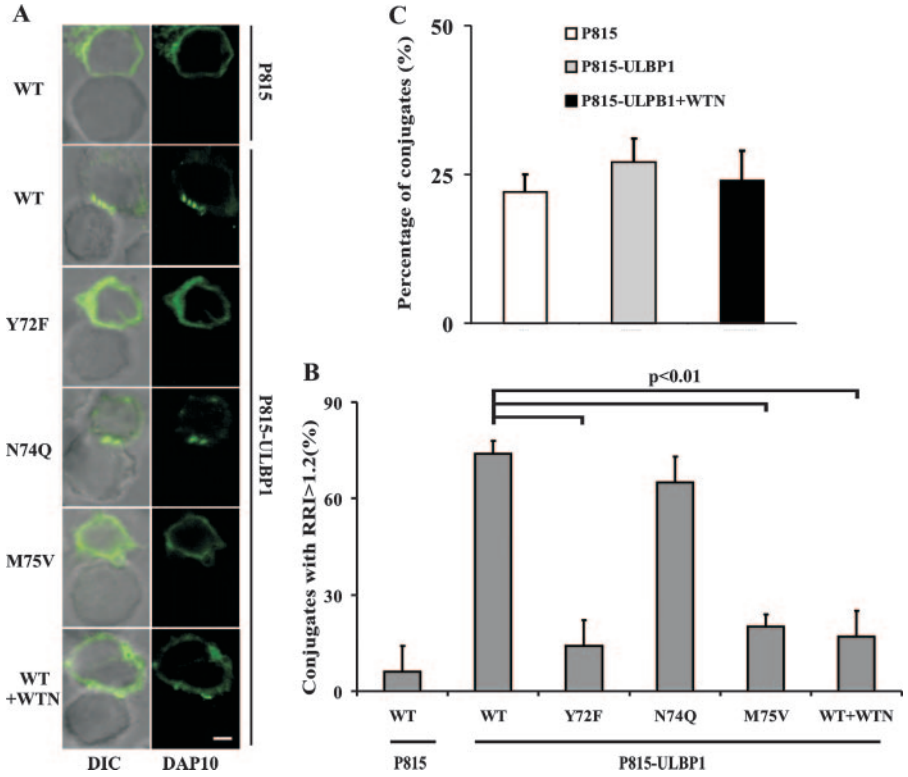

FIG. 6. Y72 and M75 residues are required for NKG2D-induced DAP10 recruitment to the NKIS. (A) Recruitment of NKG2D-DAP10 to the NKIS. NK92 cells were transduced with retroviruses expressing WT DAP10 or mutant DAP10 with mutation at Tyr-72 (Y72), Asp-74 (N74), or Met-75 (M75). Conjugates (DIC images) were examined for DAP10-YFP (green) recruitment to the contact site after conjugation with P815 or P815-ULBP1 cells for 30 min. As shown in the bottom panels, WT cells were pretreated with 100 nM WTN before conjugate formation. Bar, 5 μm. (B) Quantification of recruitment of DAP10-YFP to the NKIS, shown as the percentage of conjugates with RRIs of >1.2. Data are representative of three independent experiments. Statistical analyses were performed using paired Student's *t* test to compare the recruitment induced by the WT to that mediated by mutated chimeric receptors ($P < 0.01$). (C) Percentage of conjugates of NK92/PH(Akt)-GFP cells with the indicated target cells, with or without treatment with 100 nM WTN. Data represent mean percentages for three separate experiments. Error bars show standard deviations.

erated, with changes in the sequences encoding three critical residues. Tyrosine at position 72 was changed to phenylalanine (Y72F), asparagine at position 74 was changed to glutamine (N74Q), and methionine at position 75 was changed to valine (M75V) (Fig. 5A). Glutamine and valine were chosen because they are highly conservative changes and because these changes are known to disrupt binding to Grb2 and the p85 subunit of PI 3-kinase, respectively (33, 54). Since NKG2D surface expression is DAP10 dependent (Fig. 1B), we also confirmed the ability of each construct to assemble with NKG2D. NK92 cells expressing DAP10-YFP significantly enhanced NKG2D expression; similar expression levels of DAP10-YFP induced similar levels of NKG2D on the cell surface (Fig. 5B).

We then tested our mutants for Grb2 binding by immunoprecipitating DAP10 from cells transfected with the WT or mutated DAP10 constructs. After antibody-mediated engagement of NKG2D, DAP10-YFP immunoprecipitates were immunoblotted with antibodies to Grb2, phosphotyrosine (pY), and GFP. Grb2 was detected in immunoprecipitates of the WT constructs, demonstrating for the first time an association between Grb2 and DAP10 in cells. Mutation of both the tyrosine and asparagine residues abrogated Grb2 binding (Fig. 5C, lane 4 and lane 8). In contrast, mutation of the methionine had no effect on Grb2 binding (Fig. 5C, lane 6). Although the level of tyrosine phosphorylation in the WT and mutated DAP10 proteins was variable, we think that this was not a significant or reproducible difference.

To determine which residues are important for DAP10 recruitment to the NKIS, the NK92 cell line, transduced with a WT or mutated DAP10-YFP construct, was conjugated with P815 or P815-ULBP1 cells and imaged using confocal microscopy. While the WT construct was efficiently recruited to the NKIS, there was little to no recruitment of the Y72F or M75V construct into the NKIS (Fig. 6A and B). In contrast, the N74Q construct (Fig. 6A and B) was recruited to the NKIS with an efficiency similar to that of WT DAP10. These data indicate that residues Y72 and M75, but not N74, are important for recruitment to the NKIS.

NKG2D engagement induces PIP_3 production at the NKIS. The requirement of both the tyrosine and the methionine suggested that PI 3-kinase activation was the major signal required to induce NKG2D localization in the NKIS. To confirm a role for PI 3-kinase, human NK92 cells were treated with the PI 3-kinase inhibitor WTN. Consistent with a role for PI 3-kinase, WTN blocked recruitment of DAP10 to the NKIS

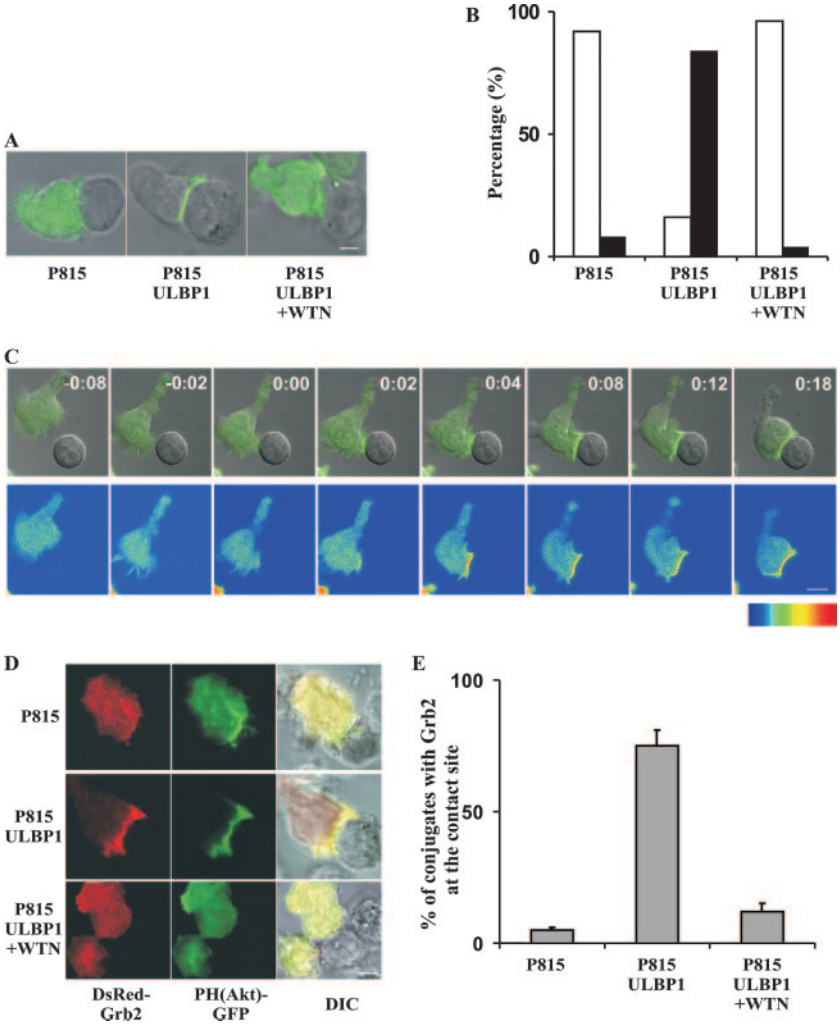

FIG. 7. NKG2D-induced PIP_3 production in the NKIS of live cells. (A) NKG2D engagement induces PIP_3 production at the NKIS. Representative images show transmitted light and fluorescence images of PH(Akt)-GFP-transduced NK92 cells conjugated with P815 or P815-ULBP1 cells. For the far right panel, transduced NK92 cells were pretreated with 100 nM WTN before being imaged. Bar, 5 μm. (B) Percentage of conjugates with PH(Akt)-GFP recruited to the NKIS. Data are shown for transduced NK92 cells showing diffuse (open) or synapse (closed) localization of PH(Akt) after conjugation with P815 or P815-ULBP1 cells in the presence or absence of WTN. Data represent three independent experiments. (C) Time-lapse experiment extracted from a movie showing a representative interaction between NK92 and P815-ULBP1 cells. (Top panels) Transmitted light and fluorescent live images of PH(Akt)-GFP-transduced NK92 cells (green) were collected every 2 s. (Bottom panels) The location of PH(Akt)-GFP is shown in false color. Bar, 5 μm. (D) Recruitment of Grb2 to the NKIS is PIP_3 dependent. Representative DIC and GFP and DsRed fluorescence images are shown for NK92 cells cotransduced with PH(Akt)-GFP and DsRed-Grb2 and conjugated with P815 or P815-ULBP1 cells after pretreatment of NK92 cells with 100 nM WTN for 15 min. Bar, 5 μm. (E) Quantitative analysis of Grb2 accumulation at the NKIS from three independent experiments with at least 50 conjugates. Data represent mean percentages of conjugates with RRIs of >1.2. Error bars show standard deviations.

(Fig. 6A and B) without affecting the ability of NK92 cells to form conjugates with target cells (Fig. 6C).

While PI 3-kinase signaling has been implicated in DAP10 signaling based on the YXXM sequence (8, 55, 59, 62), to our knowledge, direct proof that DAP10 induces PI 3-kinase activity was lacking. To confirm that PI 3-kinase was induced by DAP10, we used a biosensor to detect the presence of PIP_3, the major product of activated PI 3-kinase. The biosensor PH(Akt)-GFP binds to PIP_3, which is produced in and confined to the plasma membrane. In unstimulated cells, PH(Akt)-GFP was localized in the cytosol and nuclei of NK92 cells (data not shown). Conjugation with P815-ULBP1 cells induced a clear translocation of the biosensor to the contact site (Fig. 7A and B). No accumulation of the biosensor was observed at cell contact sites of NK cells conjugated with P815 cells alone. PIP_3 production was PI 3-kinase dependent, because treatment with the PI 3-kinase inhibitor WTN inhibited membrane translocation of PH(Akt)-GFP (Fig. 7A and B). Live cell imaging showed that PH(Akt)-GFP accumulated at the cell contact site almost immediately after conjugate formation (Fig. 7C) and appeared to spread across the contact area in a cup-like structure between the two cells.

PI 3-kinase activation is required for Grb2 recruitment to the NKIS. The lack of a requirement of the Grb2 binding site

for DAP10 recruitment to the NKIS was surprising, as recruitment of the Grb2/Vav1 complex has been shown to be required for NKG2D cytolytic activity (24, 59). We therefore considered the possibility that Grb2/Vav1 recruitment to the NKIS might not require the Grb2 binding site in DAP10. To assess the recruitment of Grb2 to the NKIS, we generated a biosensor consisting of full-length Grb2 fused to monomeric DsRed (DsRed-Grb2).

Human NK92 cells were cotransduced with both PH(Akt)-GFP and DsRed-Grb2 and then conjugated with P815-ULBP1 target cells. Recruitment of both PH(Akt)-GFP and DsRed-Grb2 occurred in a ULBP1-dependent manner (Fig. 7D and E). Surprisingly, treatment with WTN inhibited the recruitment of both biosensors to the NKIS, suggesting that Grb2 recruitment might involve PIP_3 (Fig. 7D and E). These results were confirmed using primary human NK cells incubated with anti-NKG2D-coated beads. WTN treatment blocked the recruitment of endogenous Grb2 to the contact surfaces of the beads (Fig. 8A and B). Since WTN does not affect NKG2D-initiated proximal signaling events, such as the activation of Lck (Fig. 8C) and the tyrosine phosphorylation of DAP10, Vav1, and phospholipase C-γ2 (2), this suggests that the production of PIP_3 plays a major role in controlling the membrane recruitment of Grb2.

To test the DAP10 sequence requirements for Grb2 recruitment to the NKIS, we used Flag-CD8-DAP10 chimeras to avoid stimulation of endogenous NKG2D. These chimeric receptors were generated using a Flag epitope appended to the extracellular and transmembrane portions of human CD8α, which were then fused to the cytoplasmic portion of mouse DAP10. Transduced NK92 cells were sorted to achieve a pool of cells with similar levels of CD8α surface expression (Fig. 9A). Cells were then cross-linked with anti-Flag antibodies. As expected, the WT DAP10 chimera induced PIP_3 production and Grb2 recruitment at the NKIS, while both processes were inhibited in the Y72F and M75V mutants (Fig. 9B and C). Consistent with the idea that Grb2 recruitment to the NKIS does not necessarily involve a direct physical interaction with DAP10, Grb2 was still recruited to the NKIS by the N74Q mutant, which is unable to bind Grb2 (Fig. 9B and C). These results support the idea that production of PIP_3 can explain the recruitment of Grb2 to the NKIS.

Role of YINM motif of DAP10 in NK cell lytic activity. It was possible that the Grb2 binding site was dispensable for synapse formation but required for cytolytic activity. We therefore tested the WT and mutated DAP10 constructs expressed in human transformed NK92 cells for effects on cytolysis. While untransduced NK92 cells express low levels of NKG2D and DAP10, ectopic DAP10 expression resulted in significant upregulation of NKG2D expression (Fig. 5B). Cell lines with comparable NKG2D expression were then sorted and tested for the ability to kill ULBP1-expressing target cells. While WT DAP10 resulted in a significant enhancement of target cell killing, mutation of the YXXM motif completely abrogated this effect. Surprisingly, the N74 residue was not absolutely required, as its mutation only partially reduced the enhanced killing (data not shown).

Because the interpretation of these results is complicated by the presence of endogenous DAP10 in these cells and the potential for the chimeric YFP constructs to form heterodimers with endogenous DAP10, we also used our Flag-CD8-DAP10 constructs to induce cytolysis, using anti-Flag-coated P815 cells (Fig. 9D). Consistent with the previous results, the WT construct efficiently induced NK lytic activity, while the Y72F and M75V constructs displayed poor killing of the target. Again, the N74Q mutant receptors exhibited only a moderately reduced lytic activity (Fig. 9D). These results support our finding that the YXXM motif is required for DAP10-mediated lytic activity but suggest that the YXN motif may also play a subsidiary role.

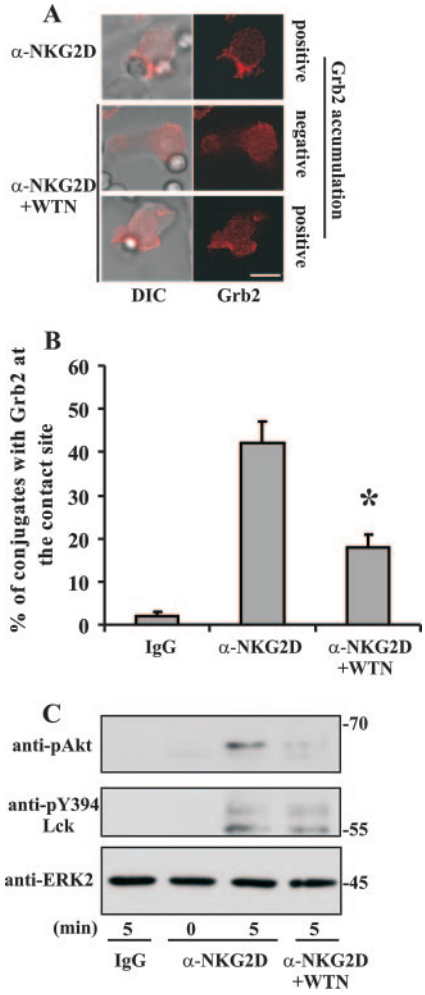

FIG. 8. Grb2 recruitment at the contact site requires PI 3-kinase activation. (A) Representative DIC and fluorescent images of Grb2 (red) after conjugation of $CD56^+$ primary human NK cells stimulated with anti-human NKG2D MAb-coated beads or mouse IgG-coated beads. Bar, 5 μm. (B) Quantitation of Grb2 accumulation at the contact site. Data represent the mean percentages of conjugates from two independent experiments. Error bars show standard deviations. The asterisk denotes that the difference is statistically significant ($P < 0.01$). (C) PI 3-kinase inhibition did not affect NKG2D-induced Lck phosphorylation. IL-2-starved $CD56^+$ human NK cells were pretreated with or without WTN and then stimulated with antibody-coated beads, as indicated. Total lysate from each sample was resolved by SDS-PAGE and stained with the indicated antibody.

Recruitment of Grb2 to the NKIS is partially mediated by the PH domain of Vav1. Since Grb2 does not contain a PH domain, what mechanism could explain the PIP_3 dependence

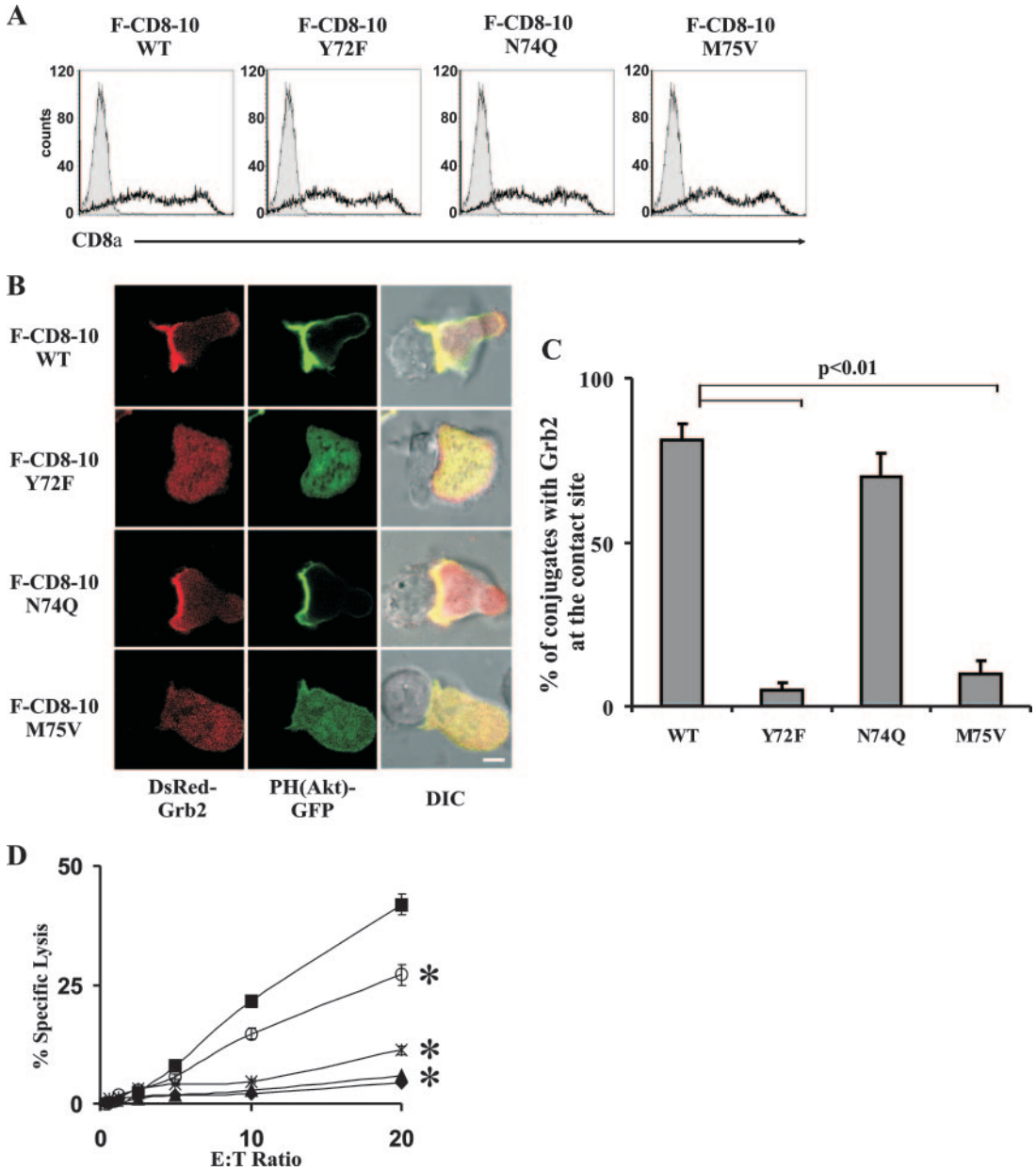

FIG. 9. Recruitment of Grb2 to the NKIS does not require the Grb2 binding site on DAP10. (A) Flow cytometric measurements of human CD8α expression on sorted NK92 cells expressing WT or mutated Flag-CD8-DAP10 chimeras (F-CD8-10). (B) NK92 cells expressing WT and mutated Flag-CD8-DAP10 chimeras were cotransduced with DsRed-Grb2 (red) and PH(Akt)-GFP (green) and then incubated with P815 cells coated with anti-Flag. Confocal images were collected 15 min after cell conjugation. Bar, 5 μm. (C) Quantification of recruitment of Grb2 to the NKIS. Data represent mean percentages of conjugates with RRIs of >1.2 from three independent experiments, with more than 50 cells analyzed in each ($P < 0.01$). (D) Redirected cytotoxicity assay of WT and mutated Flag-CD8-DAP10 constructs. NK92 cells expressing WT (closed squares), Y72F (closed triangles), N74Q (open circles), and M75V (×) chimeric receptors were incubated at the indicated effector/target (E:T) ratios with ^{51}Cr-labeled P815 cells that were preincubated with or without (diamonds) anti-Flag (10 μg/ml). Data are representative of five separate experiments. Statistical analyses were performed using paired Student's *t* test to compare the lytic activity induced by the WT to that mediated by mutated chimeric receptors ($P < 0.01$). Asterisks denote that the differences are statistically significant. Error bars show standard deviations.

of recruitment of Grb2 to the NKIS? Because two major ligands of Grb2 are Vav1 and SOS1, we considered the possibility that PH domains contained in these Grb2 ligands might explain how Grb2 is recruited to the NKIS. This hypothesis was supported by the finding that Vav1 recruitment to the NKIS was blocked by treatment with WTN (Fig. 10A and B). To confirm whether the PH domain of Vav1 was responsible, a Vav1-GFP fusion protein with two critical mutated amino acids in the PH domain was generated (26). While the WT Vav1-GFP fusion protein was efficiently recruited to the NKIS, the mutation of the PH domain only partially reduced Vav1 or Grb2 recruitment (Fig. 10C and D). Since the ability of the PH domain of Vav1 to bind to PIP_3 is unclear (30), we next tested a construct containing just the PH domain of Vav1 fused to

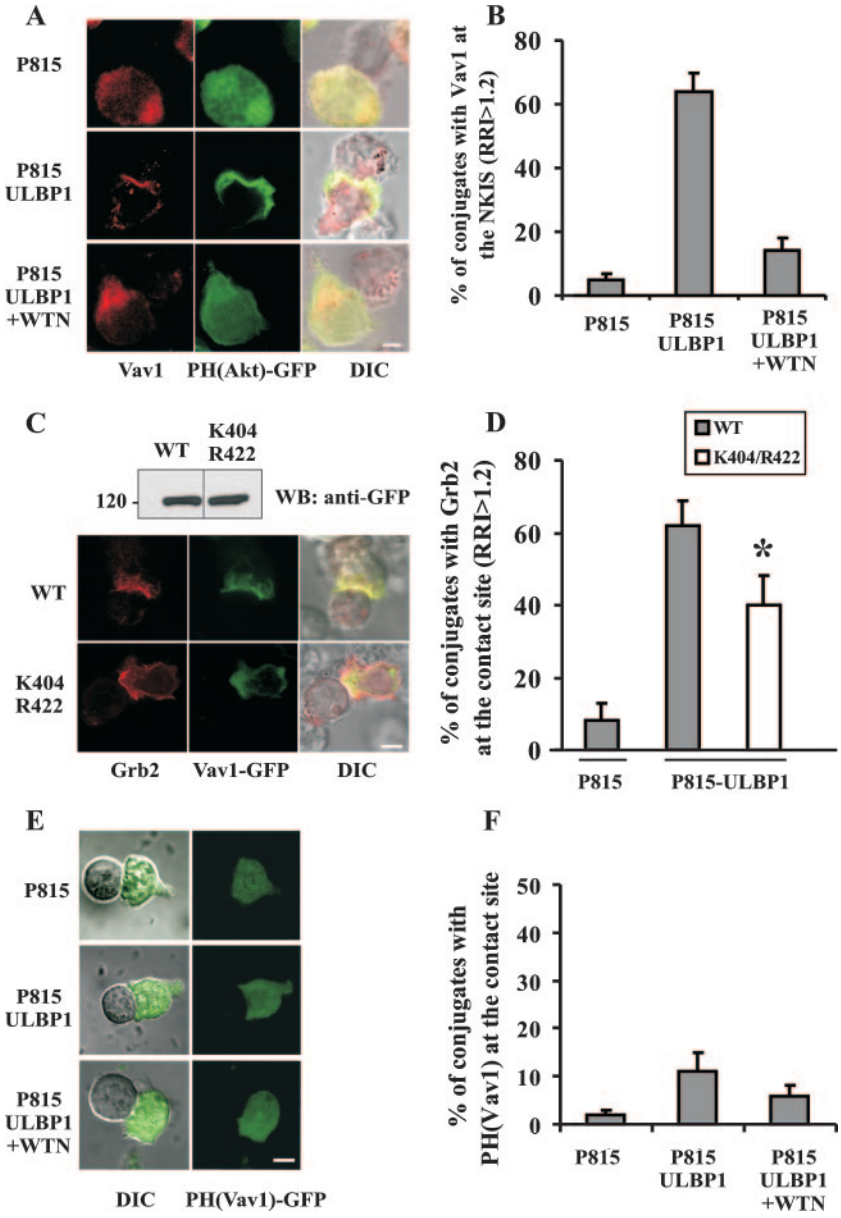

FIG. 10. Recruitment of Vav1 to the NKIS requires PI 3-kinase activation. (A) Representative DIC and fluorescent images of PH(Akt)-GFP-transduced NK92 cells conjugated with P815 cells, P815-ULBP1 cells, or P815-ULBP1 cells after pretreatment of transduced NK92 cells with 100 nM WTN for 15 min. After fixation and permeabilization, cells were stained with mouse anti-human Vav1 (red). Bar, 5 μm. (B) Quantitative analysis of Vav1 accumulation at the NKIS from three independent experiments with at least 50 conjugates. Data represent mean percentages of conjugates with RRIs of >1.2. (C) NK92 cells expressing WT or PH domain mutant (K404/R422) Vav1-GFP (green) were incubated with P815-ULBP1 cells at 37°C for 15 min. After fixation and permeabilization, cells were stained with anti-Grb2 (red). Bar, 10 μm. Anti-GFP immunoblotting was used to verify similar levels of expression of the WT and the K404/R422 mutant of Vav1-GFP. (D) Quantification of recruitment of Grb2 to the NKIS. Data represent the mean percentages of conjugates with RRIs of >1.2 from two independent experiments. The asterisk denotes that the difference is statistically significant ($P < 0.01$). (E) Representative DIC and fluorescent images of PH(Vav1)-GFP-expressing NK92 cells conjugated with P815 cells, P815-ULBP1 cells, or P815-ULBP1 cells after pretreatment with 100 nM WTN. Bar, 10 μm. (F) Quantitative analysis of PH(Vav1)-GFP translocation into the NKIS. Data represent the mean percentages of conjugates from three independent experiments with at least 50 conjugates each. Error bars show standard deviations.

GFP. While the PH(Akt) construct was readily recruited to the NKIS (Fig. 7A and B), the PH(Vav1) construct was not (Fig. 10E and F). These data demonstrate that after NKG2D engagement, the PH domain of Vav1 is not sufficient for Vav1 membrane recruitment and therefore cannot explain how Grb2 is recruited to the NKIS.

SOS1 is constitutively associated with a Grb2-Vav1 complex and is recruited to the NKIS through its PH domain. Since the other major binding partner for Grb2 is SOS1, we next tested the possibility that Grb2 recruitment to the NKIS was mediated by SOS1. A GFP fusion containing the PH domain of SOS1 was tested for the ability to be recruited to the NKIS.

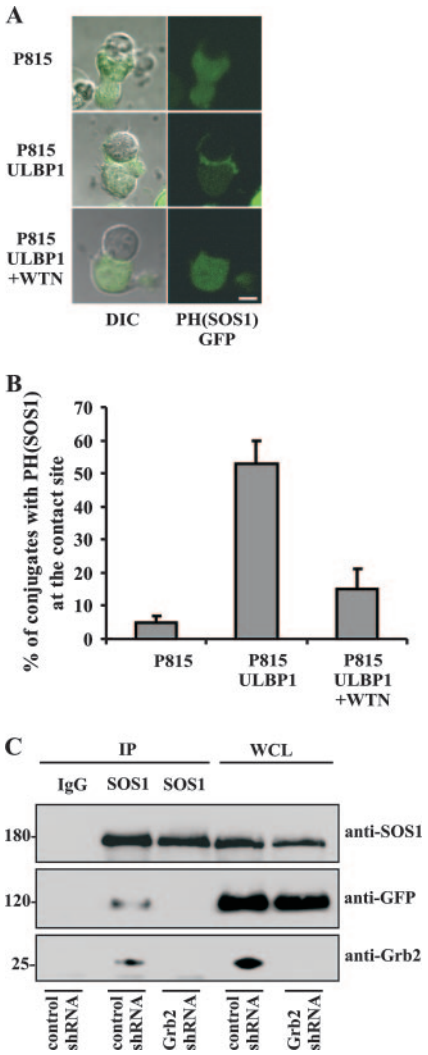

FIG. 11. SOS1 forms a complex with Grb2 and Vav1 and is recruited to the NKIS via its PH domain. (A) Representative DIC and fluorescent images of PH(SOS1)-GFP-expressing NK92 cells conjugated with P815 cells, P815-ULBP1 cells, or P815-ULBP1 cells after pretreatment with 100 nM WTN. Bar, 10 μm. (B) Quantitative analysis of PH(SOS1)-GFP translocation into the NKIS. Data represent the mean percentages of conjugates from two independent experiments. Error bars show standard deviations. (C) Grb2 is required for SOS1-Vav1 complex formation in human NK cells. Immunoprecipitates (IP) were prepared from lysates of IL-2-starved NK92/luciferase-shRNA-Vav1-GFP cells (control shRNA) or NK92/Grb2-shRNA-Vav1-GFP cells (Grb2 shRNA), using anti-SOS1 or control mouse IgG, and then immunoblotted with the indicated antibodies. Whole-cell lysates (WCL) were used to verify the Grb2 knockdown and the similar levels of expression of SOS1 and Vav1-GFP in the control and Grb2 shRNA-treated cells. Data are representative of two separate experiments.

Imaging experiments showed that the PH(SOS1) construct was efficiently recruited to the NKIS and that this recruitment was sensitive to WTN treatment (Fig. 11A and B). This indicates that PI 3-kinase activation is required for SOS1 recruitment to the NKIS and suggests that the recruitment of Grb2 to the NKIS could be mediated indirectly by the recruitment of SOS1 to the NKIS.

Since SOS1 recruitment does not readily explain how Vav1 is recruited to the NKIS, we considered the possibility that the three binding sites of Grb2 (two SH3 domains and one SH2 domain) might allow Grb2 to form large signaling complexes containing both SOS1 and Vav1. To test the requirement of Grb2 for the ability of Vav1 and SOS1 to coprecipitate together, we used an shRNA that has been used successfully to inhibit Grb2 expression (29). SOS1 immunoprecipitates prepared from NK92 cells with luciferase shRNA (shRNA control) and overexpressing Vav1-GFP contained clearly detectable Vav1 (Fig. 11C, lane 2). This suggests that Vav1 and SOS1 are associated either directly or indirectly. Importantly, in NK92 cells in which Grb2 shRNA achieved over 95% inhibition of Grb2 expression, little, if any, Vav1 was detected in SOS1 immunoprecipitates (Fig. 11C, lane 3). This suggests that the PI 3-kinase-dependent recruitment of Vav1 and Grb2 may be explained by the formation of a signaling complex containing SOS1, Vav1, and Grb2.

PI 3-kinase mediates NKG2D-induced actin polymerization, lytic granule polarization, and ERK phosphorylation. Signals transduced by NKG2D are known to induce a variety of downstream effects, including polymerization of actin, lytic granule polarization, and ERK phosphorylation (10, 24, 55). To assess actin polymerization, NK92 cells were conjugated with P815-ULBP1 cells and then stained with fluorescently labeled phalloidin. Consistent with a role for PI 3-kinase, engagement of NKG2D induced actin polymerization at the contact site (Fig. 12A and B), and this was blocked after treatment with WTN (Fig. 12A and B). We assessed the role of PI 3-kinase in lytic granule polarization by loading NK92 cells with Lysotracker and mixing them with target cells. Prior to conjugation, lytic granules were randomly distributed in the cytosol of the NK cells (data not shown). Following interaction with P815-ULBP1 cells, the granules became polarized, moving to a location near the site of contact with the target cell (Fig. 12C and D). WTN treatment blocked NKG2D-induced lytic granule polarization (Fig. 12C and D).

Lastly, we tested the dependence of ERK activation on PI 3-kinase activation. Engagement of NKG2D induced ERK1/2 phosphorylation (Fig. 12E), and treatment with WTN blocked ERK1/2 phosphorylation. Thus, multiple downstream pathways of NKG2D are dependent on PI 3-kinase activation.

DISCUSSION

NK cell killing of a target cell is a multistep process involving the formation of an NKIS, leading to lytic granule polarization and degranulation of the NK cell (3, 14, 47, 63). The existence of many different receptors involved in NK cell triggering and of different signaling pathways suggests that several different pathways may exist to regulate these changes. Here we have focused on signals mediated by DAP10. The short cytoplasmic domain contained in this non-ITAM-containing receptor allowed us to clearly dissect signals involved in immunological synapse formation for the first time.

Previously, we had shown that engagement of NKG2D could stimulate immunological synapse formation in $CD8^+$ T cells in the absence of antigen (37). Here we showed that NKG2D behaves similarly in NK cells. Extending our previous studies, we established for the first time, using a mutagenesis approach, that the organization of the NKIS induced by NKG2D is the

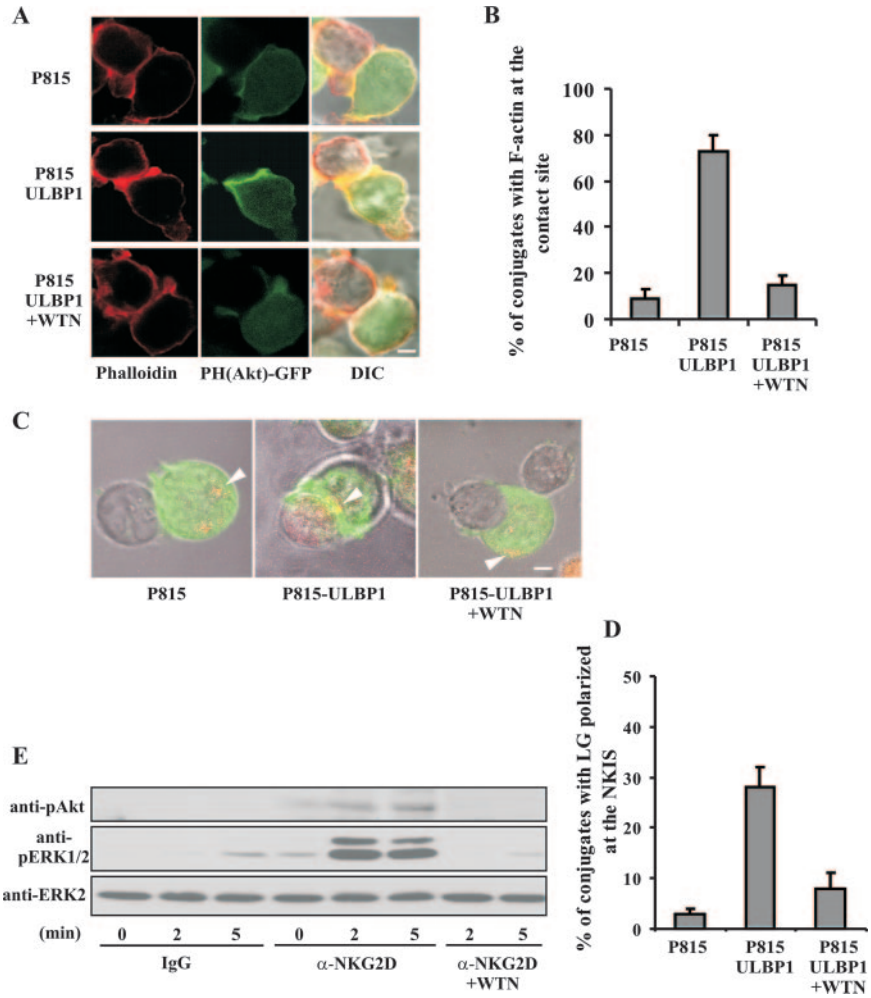

FIG. 12. Inhibition of PI 3-kinase blocks NKG2D-induced actin polymerization, lytic granule polarization, and ERK1/2 phosphorylation. (A) Representative DIC and fluorescent images of PH(Akt)-GFP-expressing NK92 cells conjugated with P815 cells, P815-ULBP1 cells, or P815-ULBP1 cells after pretreatment with 100 nM WTN. PH(Akt)-GFP is shown in green, while phalloidin-Alexa Fluor 568 staining is shown in red. Bar, 5 μm. (B) Quantitative analysis of F-actin accumulation at the NKIS from three independent experiments with at least 50 conjugates each. Data represent the mean percentages of conjugates with RRIs of >1.2. (C) Representative fluorescent images of PH(Akt)-GFP (green)-expressing NK92 cells loaded with Lysotracker (red) and conjugated with P815 cells, P815-ULBP1 cells, or P815-ULBP1 cells after pretreatment with 100 nM WTN at 37°C for 0 to 10 min. Lytic granules are indicated by arrowheads. Bar, 5 μm. (D) Quantitative analysis of lytic granule (LG) polarization at the site of contact with the indicated target cells. Data represent the mean percentages of conjugates from three independent experiments with at least 40 conjugates each. (E) PI 3-kinase inhibition blocks NKG2D-induced ERK1/2 phosphorylation. NK92 cells were IL-2 starved and then stimulated with anti-human NKG2D-coated beads or mouse IgG-coated beads for the indicated times. NK cell lysates were resolved by SDS-PAGE and probed with the indicated antibodies. Error bars show standard deviations.

result of an active process requiring signals mediated by DAP10.

Using our model system, we first determined that NKG2D signaling can occur in the absence of any other NK activating receptors. ULBP1-transfected P815 cells targeted NKG2D and DAP10 but not any other ITAM-containing adapter chains that we tested. Experiments using lipid bilayers confirmed that NKG2D could induce synapse formation by itself, as the bilayer contained only ICAM-1 and the NKG2D ligand Rae1ε. Since conjugate formation requires adhesion molecules (5), it is possible that other signals, such as those mediated by integrins, may cooperate with DAP10 signaling to mediate NKIS formation.

The YINM motif in DAP10 is similar to the YMNM motif in CD28, as it contains both a Grb2 binding site (YXN) and a PI 3-kinase binding site (YXXM). Another T-cell costimulatory molecule, ICOS, has the signaling motif YMFM and lacks the Grb2 binding site. The asparagine residue appears to be important, as the introduction of an asparagine into the ICOS signaling motif strongly enhanced the ability of ICOS to costimulate IL-2. We were therefore surprised when we found that the asparagine residue was not required for DAP10 recruitment to the NKIS. This suggests that PI 3-kinase signaling is both required and sufficient for NKG2D-mediated synapse formation.

While the presence of a YXXM motif in DAP10 had been used previously to infer the involvement of PI 3-kinase (8, 59, 62), to our knowledge direct proof that endogenous DAP10

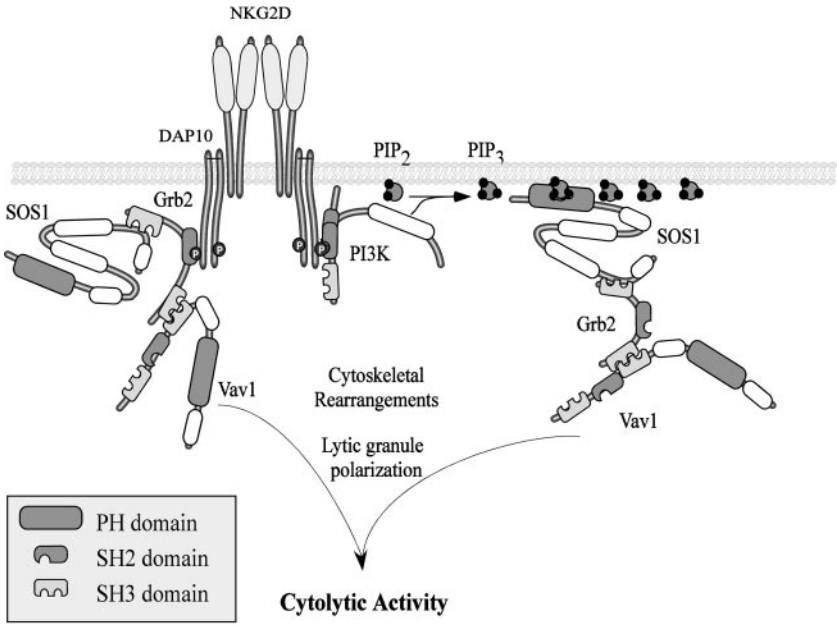

FIG. 13. Model of how the Grb2-Vav1 complex is recruited to the NKG2D synapse. As shown on the left, upon NKG2D engagement, phosphorylated DAP10 can bind to the SH2 domain of Grb2, leading to recruitment of Grb2-SOS or Grb2-Vav1 complexes. As shown on the right, recruitment of PI 3-kinase catalyzes PIP_3 production at the contact site. PIP_3 then recruits SOS1 via its PH domain to the NKG2D synapse. Through Grb2 associated with SOS1, Vav1 is also recruited.

binds to PI 3-kinase and induces production of PIP_3 in live cells had been lacking. Previous evidence for PI 3-kinase involvement consisted mainly of in vitro binding assays using the phosphorylated YXXM motif. To study DAP10-induced PI 3-kinase activation in the NKIS, we imaged the production of PIP_3 in live cells, using a biosensor consisting of GFP fused to the PH domain of Akt. We showed for the first time that NKG2D engagement induces PIP_3 production in the NKIS. Real-time images showed that PIP_3 is produced by cells within seconds of their touching the contact site, suggesting that DAP10 is phosphorylated and recruits PI 3-kinase upon engagement of NKG2D.

The product of PI 3-kinase, PIP_3, is capable of recruiting many different PH domain-containing signaling molecules, including Akt, PDK1, Itk, and phospholipase C-γ, to the plasma membrane (20, 28). While our mutagenesis studies showed that Grb2 binds to DAP10 and that this binding is disrupted by mutation of the asparagine residue, imaging experiments showed that Grb2 recruitment to the plasma membrane did not require the Grb2 binding site in DAP10 but was instead sensitive to PI 3-kinase inhibition. Our work using both biochemical and imaging approaches emphasizes the importance of using different approaches to assess the membrane recruitment of signaling proteins. The WTN sensitivity of endogenous Grb2 recruitment to the membrane by NKG2D ligation in normal human NK cells emphasizes the importance of this mechanism of recruitment.

Since Grb2 is constitutively bound to Vav1 (44, 46) and Vav1 contains a PH domain, we considered the possibility that Vav1 recruitment by PIP_3 recruits Grb2. While we found that Vav1 recruitment to the NKIS was sensitive to PI 3-kinase inhibition, the PH domain of Vav1 did not mediate the recruitment of Vav1 to the NKIS. In fact, whether the PH domain of Vav1 can bind to PIP_3 is controversial. While the PH domain of Vav1 had been shown to interact with PIP_3 (12, 26), sequence alignments led to the prediction that PIP_3 is not a physiological ligand for the PH domain of Vav1 (30). Our studies confirmed that PIP_3 is not the physiological ligand for the PH domain of Vav1.

Our studies suggest that another PH domain-containing Grb2 ligand, SOS1, is responsible for PIP_3-dependent recruitment of Grb2 to the NKIS. These data could not explain, however, why Vav1 recruitment to the NKIS was PIP_3 dependent. Since Grb2 has three potential interaction domains (two SH3 domains and one SH2 domain), we considered the possibility that Grb2 could interact with both Vav1 and SOS1 to form large complexes. This idea was supported by our data showing that the ability of Vav1 to associate with SOS1 required Grb2. This suggests that SOS1 and Vav1 exist together in a complex in human NK cells. Since SOS1 and Vav1 contain activating domains for the CDC42/Rho/Rac family of small G proteins (43), it is intriguing to speculate on the physiological roles for such a complex.

We should emphasize that our data do not imply that there is no role for the Grb2 binding site on DAP10. Rather, it seems reasonable to propose that the Grb2 binding site in DAP10 could function to stabilize or enhance the recruitment of Grb2 and Vav1 to the plasma membrane. Multiple mechanisms of recruitment for Grb2, Vav1, and SOS1 only emphasize the importance of these signaling proteins in the function of NKG2D. We should also point out that most of our experiments involved using a transformed NK cell line, i.e., NK92. While it would have been preferable to use primary NK cells, the requirement of high-efficiency cotransduction in most of our experiments precluded their use.

What is the relationship between our data determining the

requirements of DAP10 for NKIS formation and the requirements of DAP10 for cytolytic activity? Recently, Upshaw et al. showed that mutation of either the methionine or the asparagine residue impaired cytolytic activity mediated by a CD4-DAP10 fusion protein (59). Compelling experiments showed that expression of chimeric molecules fused to Grb2 and/or the p85 subunit of PI 3-kinase was required to recapitulate cytolytic activity. One interpretation of both studies together is that PI 3-kinase is required to form the NKIS but that the recruitment of Grb2 is required for cytolysis. But this interpretation is not consistent with our finding that PIP_3 production was sufficient to recruit Grb2 and Vav1 to the NKIS. It seems possible that the level or efficiency of Grb2 recruitment is different when the YXN site is mutated. It is also possible that the level of PIP_3 induced by the chimeric receptors used by Upshaw et al. (59) was lower than that in the studies described here. Further studies using measurements of PIP_3 production, as used here, and/or more physiological receptors may be necessary to determine the differences.

We propose a model in which DAP10 phosphorylation triggers PI 3-kinase activation at the contact site (Fig. 13). PIP_3 then recruits a large complex of SOS1-Grb2-Vav1 via the PH(SOS1) domain to the NKIS. Vav1 recruitment coordinates changes in the actin cytoskeleton to mediate the central recruitment of the NKG2D-DAP10 complex. The Grb2 binding site may play a secondary role to stabilize recruited Grb2 complexes at the NKIS. Thus, the activation of PI 3-kinase coupled with NKIS formation appears to play important roles in allowing for NK lytic activity.

ACKNOWLEDGMENTS

We thank J. Lin and M. Markiewicz for critically reading the manuscript. We thank M. M. Davis, D. Bar-Sagi, and W. Swat for providing reagents. We are grateful to Susan Gilfillan for helping with DAP10/DAP12^{ko} mice. We thank Aleksey Karpitskiy for technical assistance.

This work was supported by grants from NIAID.

We declare that we have no competing financial interests.

REFERENCES

1. **Bauer, S., V. Groh, J. Wu, A. Steinle, J. H. Phillips, L. L. Lanier, and T. Spies.** 1999. Activation of NK cells and T cells by NKG2D, a receptor for stress-inducible MICA. Science **285:**727–729.
2. **Billadeau, D. D., J. L. Upshaw, R. A. Schoon, C. J. Dick, and P. J. Leibson.** 2003. NKG2D-DAP10 triggers human NK cell-mediated killing via a Syk-independent regulatory pathway. Nat. Immunol. **4:**557–564.
3. **Bossi, G., C. Trambas, S. Booth, R. Clark, J. Stinchcombe, and G. M. Griffiths.** 2002. The secretory synapse: the secrets of a serial killer. Immunol. Rev. **189:**152–160.
4. **Bromley, S. K., W. R. Burack, K. G. Johnson, K. Somersalo, T. N. Sims, C. Sumen, M. M. Davis, A. S. Shaw, P. M. Allen, and M. L. Dustin.** 2001. The immunological synapse. Annu. Rev. Immunol. **19:**375–396.
5. **Bryceson, Y. T., M. E. March, H. G. Ljunggren, and E. O. Long.** 2006. Activation, coactivation, and costimulation of resting human natural killer cells. Immunol. Rev. **214:**73–91.
6. **Campbell, R. E., O. Tour, A. E. Palmer, P. A. Steinbach, G. S. Baird, D. A. Zacharias, and R. Y. Tsien.** 2002. A monomeric red fluorescent protein. Proc. Natl. Acad. Sci. USA **99:**7877–7882.
7. **Cella, M., K. Fujikawa, I. Tassi, S. Kim, K. Latinis, S. Nishi, W. Yokoyama, M. Colonna, and W. Swat.** 2004. Differential requirements for Vav proteins in DAP10- and ITAM-mediated NK cell cytotoxicity. J. Exp. Med. **200:**817–823.
8. **Chang, C., J. Dietrich, A. G. Harpur, J. A. Lindquist, A. Haude, Y. W. Loke, A. King, M. Colonna, J. Trowsdale, and M. J. Wilson.** 1999. Cutting edge: KAP10, a novel transmembrane adapter protein genetically linked to DAP12 but with unique signaling properties. J. Immunol. **163:**4651–4654.
9. **Chardin, P., J. H. Camonis, N. W. Gale, L. van Aelst, J. Schlessinger, M. H. Wigler, and D. Bar-Sagi.** 1993. Human Sos1: a guanine nucleotide exchange factor for Ras that binds to GRB2. Science **260:**1338–1343.
10. **Chen, X., P. P. Trivedi, B. Ge, K. Krzewski, and J. L. Strominger.** 2007. Many NK cell receptors activate ERK2 and JNK1 to trigger microtubule organizing center and granule polarization and cytotoxicity. Proc. Natl. Acad. Sci. USA **104:**6329–6334.
11. **Cosman, D., J. Mullberg, C. L. Sutherland, W. Chin, R. Armitage, W. Fanslow, M. Kubin, and N. J. Chalupny.** 2001. ULBPs, novel MHC class I-related molecules, bind to CMV glycoprotein UL16 and stimulate NK cytotoxicity through the NKG2D receptor. Immunity **14:**123–133.
12. **Das, B., X. Shu, G. J. Day, J. Han, U. M. Krishna, J. R. Falck, and D. Broek.** 2000. Control of intramolecular interactions between the pleckstrin homology and Dbl homology domains of Vav and Sos1 regulates Rac binding. J. Biol. Chem. **275:**15074–15081.
13. **Davis, D. M.** 2002. Assembly of the immunological synapse for T cells and NK cells. Trends Immunol. **23:**356–363.
14. **Davis, D. M., I. Chiu, M. Fassett, G. B. Cohen, O. Mandelboim, and J. L. Strominger.** 1999. The human natural killer cell immune synapse. Proc. Natl. Acad. Sci. USA **96:**15062–15067.
15. **Davis, D. M., and M. L. Dustin.** 2004. What is the importance of the immunological synapse? Trends Immunol. **25:**323–327.
16. **Diefenbach, A., E. Tomasello, M. Lucas, A. M. Jamieson, J. K. Hsia, E. Vivier, and D. H. Raulet.** 2002. Selective associations with signaling proteins determine stimulatory versus costimulatory activity of NKG2D. Nat. Immunol. **3:**1142–1149.
17. **Doubrovina, E. S., M. M. Doubrovin, E. Vider, R. B. Sisson, R. J. O'Reilly, B. Dupont, and Y. M. Vyas.** 2003. Evasion from NK cell immunity by MHC class I chain-related molecules expressing colon adenocarcinoma. J. Immunol. **171:**6891–6899.
18. **Dustin, M. L., M. W. Olszowy, A. D. Holdorf, J. Li, S. Bromley, N. Desai, P. Widder, F. Rosenberger, P. A. van der Merwe, P. M. Allen, and A. S. Shaw.** 1998. A novel adaptor protein orchestrates receptor patterning and cytoskeletal polarity in T-cell contacts. Cell **94:**667–677.
19. **Endt, J., F. E. McCann, C. R. Almeida, D. Urlaub, R. Leung, D. Pende, D. M. Davis, and C. Watzl.** 2007. Inhibitory receptor signals suppress ligation-induced recruitment of NKG2D to GM1-rich membrane domains at the human NK cell immune synapse. J. Immunol. **178:**5606–5611.
20. **Falasca, M., S. K. Logan, V. P. Lehto, G. Baccante, M. A. Lemmon, and J. Schlessinger.** 1998. Activation of phospholipase C gamma by PI 3-kinase-induced PH domain-mediated membrane targeting. EMBO J. **17:**414–422.
21. **Garrity, D., M. E. Call, J. Feng, and K. W. Wucherpfennig.** 2005. The activating NKG2D receptor assembles in the membrane with two signaling dimers into a hexameric structure. Proc. Natl. Acad. Sci. USA **102:**7641–7646.
22. **Gasser, S., S. Orsulic, E. J. Brown, and D. H. Raulet.** 2005. The DNA damage pathway regulates innate immune system ligands of the NKG2D receptor. Nature **436:**1186–1190.
23. **Gilfillan, S., E. L. Ho, M. Cella, W. M. Yokoyama, and M. Colonna.** 2002. NKG2D recruits two distinct adapters to trigger NK cell activation and costimulation. Nat. Immunol. **3:**1150–1155.
24. **Graham, D. B., M. Cella, E. Giurisato, K. Fujikawa, A. V. Miletic, T. Kloeppel, K. Brim, T. Takai, A. S. Shaw, M. Colonna, and W. Swat.** 2006. Vav1 controls DAP10-mediated natural cytotoxicity by regulating actin and microtubule dynamics. J. Immunol. **177:**2349–2355.
25. **Grakoui, A., S. K. Bromley, C. Sumen, M. M. Davis, A. S. Shaw, P. M. Allen, and M. L. Dustin.** 1999. The immunological synapse: a molecular machine controlling T cell activation. Science **285:**221–227.
26. **Han, J., K. Luby-Phelps, B. Das, X. Shu, Y. Xia, R. D. Mosteller, U. M. Krishna, J. R. Falck, M. A. White, and D. Broek.** 1998. Role of substrates and products of PI 3-kinase in regulating activation of Rac-related guanosine triphosphatases by Vav. Science **279:**558–560.
27. **Harada, Y., D. Ohgai, R. Watanabe, K. Okano, O. Koiwai, K. Tanabe, H. Toma, A. Altman, and R. Abe.** 2003. A single amino acid alteration in cytoplasmic domain determines IL-2 promoter activation by ligation of CD28 but not inducible costimulator (ICOS). J. Exp. Med. **197:**257–262.
28. **Hemmings, B. A.** 1997. PH domains—a universal membrane adapter. Science **275:**1899.
29. **Huang, F., and A. Sorkin.** 2005. Growth factor receptor binding protein 2-mediated recruitment of the RING domain of Cbl to the epidermal growth factor receptor is essential and sufficient to support receptor endocytosis. Mol. Biol. Cell **16:**1268–1281.
30. **Isakoff, S. J., T. Cardozo, J. Andreev, Z. Li, K. M. Ferguson, R. Abagyan, M. A. Lemmon, A. Aronheim, and E. Y. Skolnik.** 1998. Identification and analysis of PH domain-containing targets of phosphatidylinositol 3-kinase using a novel in vivo assay in yeast. EMBO J. **17:**5374–5387.
31. **Kaifu, T., J. Nakahara, M. Inui, K. Mishima, T. Momiyama, M. Kaji, A. Sugahara, H. Koito, A. Ujike-Asai, A. Nakamura, K. Kanazawa, K. Tan-Takeuchi, K. Iwasaki, W. M. Yokoyama, A. Kudo, M. Fujiwara, H. Asou, and T. Takai.** 2003. Osteopetrosis and thalamic hypomyelinosis with synaptic degeneration in DAP12-deficient mice. J. Clin. Investig. **111:**323–332.
32. **Khurana, D., L. N. Arneson, R. A. Schoon, C. J. Dick, and P. J. Leibson.** 2007. Differential regulation of human NK cell-mediated cytotoxicity by the tyrosine kinase itk. J. Immunol. **178:**3575–3582.
33. **Kim, H. H., M. Tharayil, and C. E. Rudd.** 1998. Growth factor receptor-

bound protein 2 SH2/SH3 domain binding to CD28 and its role in co-signaling. J. Biol. Chem. **273:**296–301.
34. **Lanier, L. L.** 2003. Natural killer cell receptor signaling. Curr. Opin. Immunol. **15:**308–314.
35. **Lanier, L. L., B. C. Corliss, J. Wu, C. Leong, and J. H. Phillips.** 1998. Immunoreceptor DAP12 bearing a tyrosine-based activation motif is involved in activating NK cells. Nature **391:**703–707.
36. **Long, E. O.** 2002. Tumor cell recognition by natural killer cells. Semin. Cancer Biol. **12:**57–61.
37. **Markiewicz, M. A., L. N. Carayannopoulos, O. V. Naidenko, K. Matsui, W. R. Burack, E. L. Wise, D. H. Fremont, P. M. Allen, W. M. Yokoyama, M. Colonna, and A. S. Shaw.** 2005. Costimulation through NKG2D enhances murine CD8+ CTL function: similarities and differences between NKG2D and CD28 costimulation. J. Immunol. **175:**2825–2833.
38. **Masilamani, M., C. Nguyen, J. Kabat, F. Borrego, and J. E. Coligan.** 2006. CD94/NKG2A inhibits NK cell activation by disrupting the actin network at the immunological synapse. J. Immunol. **177:**3590–3596.
39. **Meresse, B., Z. Chen, C. Ciszewski, M. Tretiakova, G. Bhagat, T. N. Krausz, D. H. Raulet, L. L. Lanier, V. Groh, T. Spies, E. C. Ebert, P. H. Green, and B. Jabri.** 2004. Coordinated induction by IL15 of a TCR-independent NKG2D signaling pathway converts CTL into lymphokine-activated killer cells in celiac disease. Immunity **21:**357–366.
40. **Micucci, F., A. Zingoni, M. Piccoli, L. Frati, A. Santoni, and R. Galandrini.** 2006. High-efficient lentiviral vector-mediated gene transfer into primary human NK cells. Exp. Hematol. **34:**1344–1352.
41. **Moretta, A., C. Bottino, M. Vitale, D. Pende, C. Cantoni, M. C. Mingari, R. Biassoni, and L. Moretta.** 2001. Activating receptors and coreceptors involved in human natural killer cell-mediated cytolysis. Annu. Rev. Immunol. **19:**197–223.
42. **Nedvetzki, S., S. Sowinski, R. A. Eagle, J. Harris, F. Vely, D. Pende, J. Trowsdale, E. Vivier, S. Gordon, and D. M. Davis.** 2007. Reciprocal regulation of natural killer cells and macrophages associated with distinct immune synapses. Blood **109:**3776–3785.
43. **Nimnual, A., and D. Bar-Sagi.** 2002. The two hats of SOS. Sci. STKE **2002:**PE36.
44. **Nishida, M., K. Nagata, Y. Hachimori, M. Horiuchi, K. Ogura, V. Mandiyan, J. Schlessinger, and F. Inagaki.** 2001. Novel recognition mode between Vav and Grb2 SH3 domains. EMBO J. **20:**2995–3007.
45. **Nosaka, T., T. Kawashima, K. Misawa, K. Ikuta, A. L. Mui, and T. Kitamura.** 1999. STAT5 as a molecular regulator of proliferation, differentiation and apoptosis in hematopoietic cells. EMBO J. **18:**4754–4765.
46. **Ogura, K., K. Nagata, M. Horiuchi, E. Ebisui, T. Hasuda, S. Yuzawa, M. Nishida, H. Hatanaka, and F. Inagaki.** 2002. Solution structure of N-terminal SH3 domain of Vav and the recognition site for Grb2 C-terminal SH3 domain. J. Biomol. NMR **22:**37–46.
47. **Orange, J. S., K. E. Harris, M. M. Andzelm, M. M. Valter, R. S. Geha, and J. L. Strominger.** 2003. The mature activating natural killer cell immunologic synapse is formed in distinct stages. Proc. Natl. Acad. Sci. USA **100:**14151–14156.
48. **Pende, D., P. Rivera, S. Marcenaro, C. C. Chang, R. Biassoni, R. Conte, M. Kubin, D. Cosman, S. Ferrone, L. Moretta, and A. Moretta.** 2002. Major histocompatibility complex class I-related chain A and UL16-binding protein expression on tumor cell lines of different histotypes: analysis of tumor susceptibility to NKG2D-dependent natural killer cell cytotoxicity. Cancer Res. **62:**6178–6186.
49. **Prasad, K. V., Y. C. Cai, M. Raab, B. Duckworth, L. Cantley, S. E. Shoelson, and C. E. Rudd.** 1994. T-cell antigen CD28 interacts with the lipid kinase phosphatidylinositol 3-kinase by a cytoplasmic Tyr(P)-Met-Xaa-Met motif. Proc. Natl. Acad. Sci. USA **91:**2834–2838.
50. **Raulet, D. H.** 2003. Roles of the NKG2D immunoreceptor and its ligands. Nat. Rev. Immunol. **3:**781–790.
51. **Richie, L. I., P. J. Ebert, L. C. Wu, M. F. Krummel, J. J. Owen, and M. M. Davis.** 2002. Imaging synapse formation during thymocyte selection: inability of CD3zeta to form a stable central accumulation during negative selection. Immunity **16:**595–606.
52. **Roda-Navarro, P., M. Vales-Gomez, S. E. Chisholm, and H. T. Reyburn.** 2006. Transfer of NKG2D and MICB at the cytotoxic NK cell immune synapse correlates with a reduction in NK cell cytotoxic function. Proc. Natl. Acad. Sci. USA **103:**11258–11263.
53. **Somersalo, K., N. Anikeeva, T. N. Sims, V. K. Thomas, R. K. Strong, T. Spies, T. Lebedeva, Y. Sykulev, and M. L. Dustin.** 2004. Cytotoxic T lymphocytes form an antigen-independent ring junction. J. Clin. Investig. **113:**49–57.
54. **Songyang, Z., S. E. Shoelson, M. Chaudhuri, G. Gish, T. Pawson, W. G. Haser, F. King, T. Roberts, S. Ratnofsky, R. J. Lechleider, et al.** 1993. SH2 domains recognize specific phosphopeptide sequences. Cell **72:**767–778.
55. **Sutherland, C. L., N. J. Chalupny, K. Schooley, T. VandenBos, M. Kubin, and D. Cosman.** 2002. UL16-binding proteins, novel MHC class I-related proteins, bind to NKG2D and activate multiple signaling pathways in primary NK cells. J. Immunol. **168:**671–679.
56. **Taylor, L. S., S. P. Paul, and D. W. McVicar.** 2000. Paired inhibitory and activating receptor signals. Rev. Immunogenet. **2:**204–219.
57. **Tomasello, E., and E. Vivier.** 2005. KARAP/DAP12/TYROBP: three names and a multiplicity of biological functions. Eur. J. Immunol. **35:**1670–1677.
58. **Treanor, B., P. M. Lanigan, S. Kumar, C. Dunsby, I. Munro, E. Auksorius, F. J. Culley, M. A. Purbhoo, D. Phillips, M. A. Neil, D. N. Burshtyn, P. M. French, and D. M. Davis.** 2006. Microclusters of inhibitory killer immunoglobulin-like receptor signaling at natural killer cell immunological synapses. J. Cell Biol. **174:**153–161.
59. **Upshaw, J. L., L. N. Arneson, R. A. Schoon, C. J. Dick, D. D. Billadeau, and P. J. Leibson.** 2006. NKG2D-mediated signaling requires a DAP10-bound Grb2-Vav1 intermediate and phosphatidylinositol-3-kinase in human natural killer cells. Nat. Immunol. **7:**524–532.
60. **Vyas, Y. M., H. Maniar, and B. Dupont.** 2002. Visualization of signaling pathways and cortical cytoskeleton in cytolytic and noncytolytic natural killer cell immune synapses. Immunol. Rev. **189:**161–178.
61. **Wu, J., H. Cherwinski, T. Spies, J. H. Phillips, and L. L. Lanier.** 2000. DAP10 and DAP12 form distinct, but functionally cooperative, receptor complexes in natural killer cells. J. Exp. Med. **192:**1059–1068.
62. **Wu, J., Y. Song, A. B. Bakker, S. Bauer, T. Spies, L. L. Lanier, and J. H. Phillips.** 1999. An activating immunoreceptor complex formed by NKG2D and DAP10. Science **285:**730–732.
63. **Wulfing, C., B. Purtic, J. Klem, and J. D. Schatzle.** 2003. Stepwise cytoskeletal polarization as a series of checkpoints in innate but not adaptive cytolytic killing. Proc. Natl. Acad. Sci. USA **100:**7767–7772.
64. **Yokoyama, W. M., and B. F. Plougastel.** 2003. Immune functions encoded by the natural killer gene complex. Nat. Rev. Immunol. **3:**304–316.
65. **Zompi, S., J. A. Hamerman, K. Ogasawara, E. Schweighoffer, V. L. Tybulewicz, J. P. Di Santo, L. L. Lanier, and F. Colucci.** 2003. NKG2D triggers cytotoxicity in mouse NK cells lacking DAP12 or Syk family kinases. Nat. Immunol. **4:**565–572.